

NASA Contractor Report 158893

MODEL 340 MAIN FIXED AND MOVABLE CONTROL SURFACE
FLUTTER ANALYSIS

(NASA-CR-158893) MODEL 340 MAIN FIXED AND
MOVABLE CONTROL SURFACE FLUTTER ANALYSIS
(Consolidated Vultee Aircraft Corp.) 47 p

N78-77722

00/08 **Unclas**
 25886

C. D. Pancu and K. Hiroshige

CONSOLIDATED VULTEE AIRCRAFT CORPORATION
San Diego, CA

August 28, 1951

NASA

National Aeronautics and
Space Administration

Langley Research Center
Hampton, Virginia 23665



DESIGNED BY
CHECKED BY
APPROVED BY
DATE

CONSOLIDATED VULTURE AIRCRAFT CORPORATION
SAN DIEGO DIVISION

PAGE 11
REPORT NO. ZU-
MODEL 340
DATE 11-1-50

PREFACE

This analysis is submitted in fulfillment of Civil Air Regulations Airplane Airworthiness part 4a, sec. #308 for model #340. The calculations are made for the version of this airplane which will use an Allison turbo-prop engine; as this model has approximately the same level flight and diving speeds as the #340 with a conventional reciprocating engine it is considered that this analysis also applies to the latter model which has similar mass and stiffness distributions for the main structure of wing, fuselage and tail surfaces.

SUMMARY

The results of a flutter investigation for the main fixed and movable control surfaces of the version of the airplane model #340 using an Allison turbo-prop engine are as follows:

Cond.	Flutter mode	V_F (MPH)	Ref.
1	Maximum Gross Weight (53,200 lbs.) Symmetric first coupled wing mode (22.9 rad/sec.) - symmetric second coupled wing mode (36.8 rad/sec.) - aileron rotation (0 rad/sec.)	Stable $g = -.041$ $V_F = 570$	Fig. 7
2	Maximum Gross Weight Symmetric first coupled wing mode (22.9 rad/sec.) - symmetric second coupled wing mode (36.8 rad/sec.)	Stable $g = -.132$ $V_F = 570$	Fig. 7
3	Maximum Gross Weight Antisymmetric first coupled wing mode (29.8 rad/sec.) - antisymmetric second coupled wing mode (48.0 rad/sec.) - aileron rotation (0 rad/sec.)	Stable $g = -.220$ $V_F = 570$	Fig. 8
4	Maximum Gross Weight Antisymmetric first coupled wing mode (29.8 rad/sec.) - antisymmetric second coupled wing mode (48.0 rad/sec.)	Stable $g = -.051$ $V_F = 570$	Fig. 8
5	Minimum Gross Weight (28,630 lbs.) Symmetric first coupled wing mode (22.9 rad/sec.) - symmetric second coupled wing mode (36.8 rad/sec.) - aileron rotation (0 rad/sec.)	Stable $g = -.035$ $V_F = 570$	Fig. 9
6	Minimum Gross Weight Symmetric first coupled wing mode (22.9 rad/sec.) - symmetric second coupled wing mode (36.8 rad/sec.)	Stable $g = -.105$ $V_F = 570$	Fig. 9
7	Minimum Gross Weight Antisymmetric first coupled wing mode (29.8 rad/sec.) - antisymmetric second coupled wing mode (48.0 rad/sec.) - aileron rotation (0 rad/sec.)	Stable $g = -.232$ $V_F = 570$	Fig. 10
8	Minimum Gross Weight Antisymmetric first coupled wing mode (29.8 rad/sec.) - antisymmetric second couple wing mode (48.0 rad/sec.)	Stable $g = -.207$ $V_F = 570$	Fig. 10
9	Maximum Gross Weight Fuselage (41,550 lbs.) Lateral first coupled fuselage mode (37.0 rad/sec.) - lateral second coupled fuselage mode (56.0 rad/sec.) - rudder rotation (0 rad/sec.)	Stable $g = -.092$ $V_F = 570$	Fig. 11

SECONDARY (Cont'd.)

Cond.	Flutter mode	* U_F (MPH)	Ref.
10	Horizontal Tail Cantilevered first coupled mode (35.8 rad/sec.)- cantilevered second coupled mode (141.0 rad/sec.)- elevator rotation (0 rad/sec.)	620	Fig. 11
11	Horizontal Tail Cantilevered first coupled mode (35.8 rad/sec.)- cantilevered second coupled mode (141.0 rad/sec.)	Stable $g = -.39$ $@ U_F = 570$	Fig. 11
12	Vertical Tail Cantilevered first coupled mode (66.5 rad/sec.)- cantilevered second coupled mode (144.0 rad/sec.)- rudder rotation (0 rad/sec.)	673	Fig. 11
13	Vertical Tail Cantilevered first coupled mode (66.5 rad/sec.)- cantilevered second coupled mode (144.0 rad/sec.)	Stable $g = -.265$ $@ U_F = 570$	Fig. 11

* U_F = True flutter speed (speed for zero structural damping coefficient) at 10,000 ft. altitude, corrected for compressibility by the method of Reference 1, 2, given unless no flutter speed was determined in which case the margin of structural damping coefficient is given at the required flutter speed.

g = Damping coefficient of structure required for neutral stability.

The above results indicate that the main wing and tail surfaces are stable at 570 mph which is the required true flutter speed (20% over limit dive speed at 10,000 ft.)

$$V_{LD} = 475 \text{ mph TAS}$$

INTRODUCTION

Flutter calculations are made in this report for the Model 340 airplane which is the version using the Allison turbo-propeller engine.

The calculations are made at a 10,000 foot altitude using the following coupled vibration modes:

- Cond. 1. Maximum Gross Weight (53,200 lbs.)
Symmetric first coupled wing mode (22.9 rad./sec.) -
symmetric second coupled wing mode (36.8 rad./sec.) -
aileron rotation (0 rad./sec.)
- Cond. 2. Maximum Gross Weight
Symmetric first coupled wing mode (22.9 rad/sec.) - symmetric
second coupled wing mode (36.8 rad./sec.)
- Cond. 3. Maximum Gross Weight
Antisymmetric first coupled wing mode (29.8 rad./sec.) -
antisymmetric
second coupled wing mode (48.0 rad/sec.) - aileron
rotation (0 rad/sec.)
- Cond. 4. Maximum Gross Weight
Antisymmetric first coupled wing mode (29.8 rad/sec) -
antisymmetric second coupled wing mode (48.0 rad/sec.)
- Cond. 5. Minimum Gross Weight (28,630 lbs.)
Symmetric first coupled wing mode (22.9 rad/sec.) -
symmetric second coupled wing mode (36.8 rad/sec.) -
aileron rotation (0 rad/sec.)
- Cond. 6. Minimum Gross Weight
Symmetric first coupled wing mode (22.9 rad/sec.) -
symmetric second coupled wing mode (36.8 rad/sec.)
- Cond. 7. Minimum Gross Weight
Antisymmetric first coupled wing mode (29.8 rad/sec.) -
antisymmetric second coupled wing mode (48.0 rad/sec.) -
aileron rotation (0 rad/sec.)
- Cond. 8. Minimum Gross Weight
Antisymmetric first coupled wing mode (29.8 rad/sec.) -
antisymmetric second coupled wing mode (48.0 rad/sec.)
- Cond. 9. Maximum Gross Weight Fuselage (41,550 lbs.)
Lateral first coupled fuselage mode (37.0 rad/sec.) -
lateral second coupled fuselage mode (56.0 rad/sec.) -
rudder rotation (0 rad/sec.)

- Cond. 10. Horizontal Tail
Cantilevered first coupled mode (35.8 rad/sec.) -
cantilevered second coupled mode (141.0 rad/sec.) -
elevator rotation (0 rad/sec.)
- Cond. 11. Horizontal Tail
Cantilevered first coupled mode (35.8 rad/sec.) -
cantilevered second coupled mode (141.0 rad/sec.)
- Cond. 12. Vertical Tail
Cantilevered first coupled mode (66.5 rad/sec.) -
cantilevered second coupled mode (144.0 rad/sec.) -
rudder rotation (0 rad/sec.)
- Cond. 13. Vertical Tail
Cantilevered first coupled mode (66.5 rad/sec.) -
cantilevered second coupled mode (144.0 rad/sec.)

The notation used in this report is the same as in Reference 1
except as noted otherwise herein.

Planform Dimensions, Mass and Stiffness Data

Figures 1 and 2 respectively present sketches of the wing and fuselage showing the elastic axes of these airplane components with the station locations at which the masses are concentrated for the calculation of the vibration modes. Tables I and II present the mass data corresponding to these stations as well as the wing strip widths used in determining the aerodynamic forces and moments on each mass. It is to be noted that the aileron mass was assumed to be concentrated at one station as shown in figure 1, but the aerodynamic forces and moments were based on the wing strip widths of the wing section at the aileron. Figures 3 and 4 respectively show the stiffness distributions along the wing and fuselage elastic axes from which the wing and fuselage elastic coefficients (as defined in Reference 2) presented in Table III were determined for each of the corresponding wing and fuselage stations.

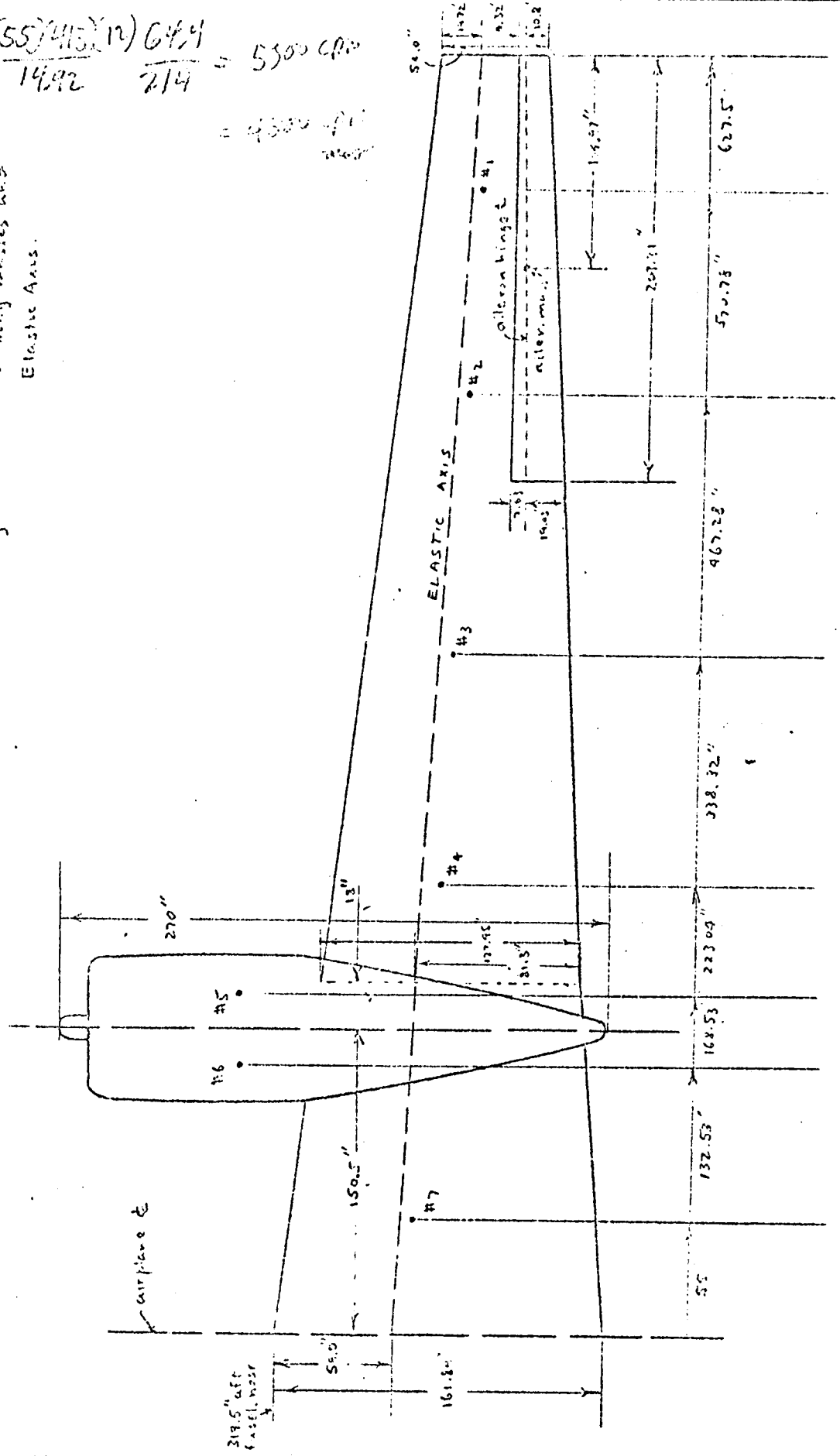
Figure 5 shows a sketch of the vertical and horizontal tail surfaces showing the elastic axes and stations of mass concentration for the calculation of the vibration modes. Table IV presents the mass data corresponding to these stations on the horizontal and vertical tail with the wing strip widths used in determining the aerodynamic forces and moments. Table V presents the elastic coefficients (as defined in Reference 2) for the tail surfaces, based on the stiffness distributions shown in Figure 6.

The rotational stiffness of all of the control surfaces, i.e., aileron, elevator, and rudder, was assumed to be zero.

$$w = \frac{(55)(415)(12)(64.4)}{14.92} \cdot \frac{1}{214} = 5300 \text{ CPD}$$

$$= 4300 \text{ CPD}$$

Fig. 1. Location of wing masses and Elastic Axis.



19.53
 10.5
 3.23
 4.12
 12.0
 14.12

FIGURE 2
 FUSELAGE MASS STATIONS AND FUSELAGE ELASTIC AXIS

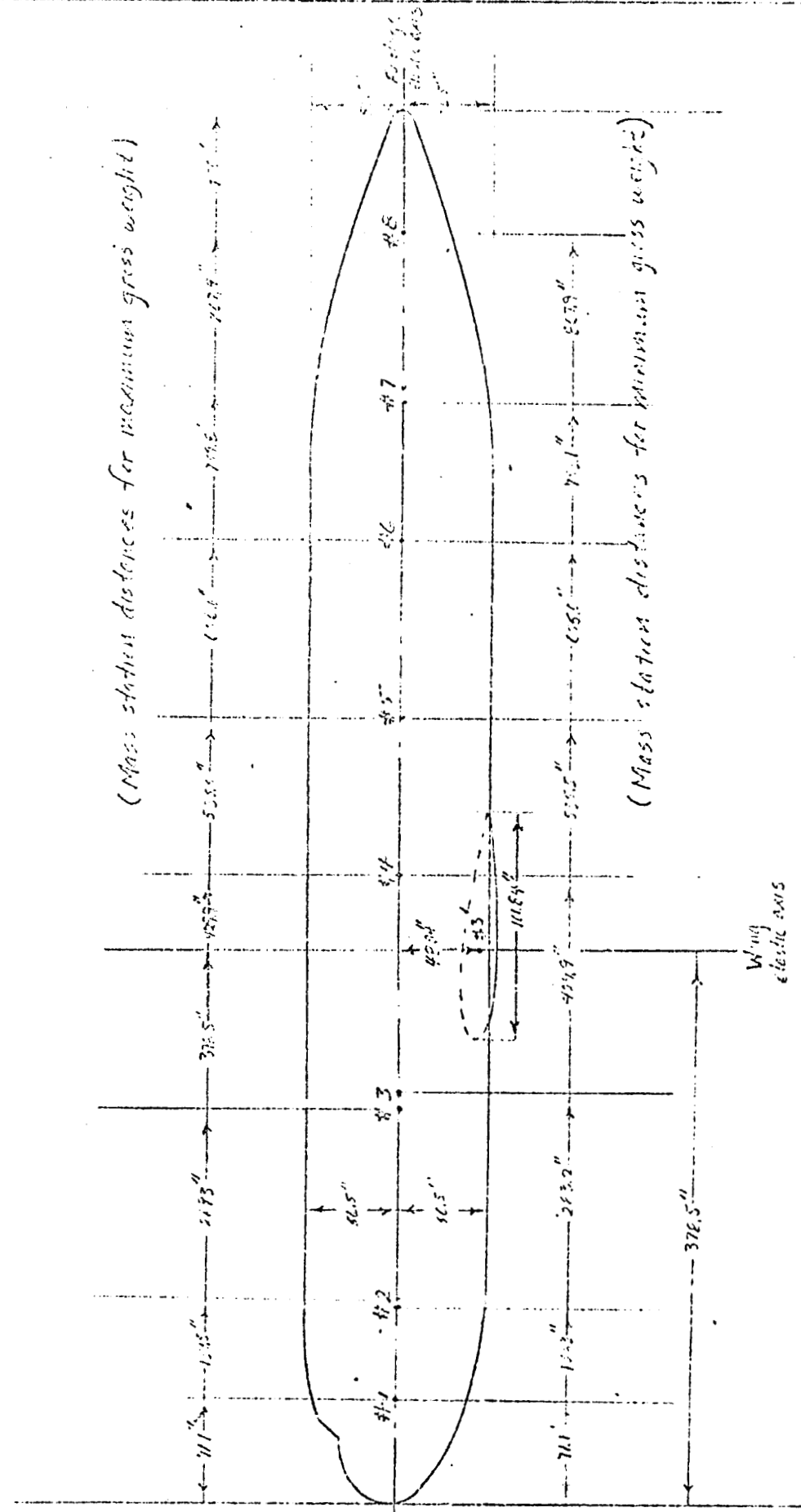


TABLE I

MASS DISTRIBUTION OF WING AND FUSELAGE
PER
MAXIMUM GROSS WEIGHT (53,000 LBS.) CONFIGURE

Wing Mass Distribution (per side, incl. ailer.)

Wing Sta.	Dist. to Fuselage \pm (in.)	Mass (slug)	Mass Unbalance* (slug ft.)	Mass Mom. of Inertia about Elastic Axis (slug ft. ²)	Wing Strip Width (in.)
1	576.70	3.40	2.1652	0.62	104.97
2	467.20	27.63	4.329	32.46	104.97
3	336.32	27.7	10.824	13.3	140.36
4	223.00	19.40	7.2017	177.9	10.71
5	167.52	10.2	-11.25	61.0	36.0
6	132.55	14.08	-609.64	610	36.0
7	59.60	20.35	12.199	183.2	39.53

* Positive for mass center of gravity aft of wing elastic axis.

Aileron Mass Distribution (per side)

Aileron Sta.	Dist. to Fuselage \pm (in.)	Mass (slug)	Mass Unbalance (slug ft.)	Mass Mom. of Inertia about (slug ft. ²)	Wing Strip Width (ft.)
1'	528.5	2.64	0	0.625	**

** Wing strip widths for stations 1 and 2 are used for the aerodynamic loading computations.

Table 1-Cont'd.

Fuselage Mass Distribution (per side, incl. top surface)

Fuse Sta.	Dist. aft of Fuse nose (in.)	Mass (slugs)	Mass Balance ** (slug ft.)	Mass Mom. of Inertia about Elastic axis (slug ft. ²)
1	71.1	32.81	0	222.0
2	139.5	37.55	0	533.5
3	202.3	113.7	0	1,441
3*	372.5	234.84	957.75	69,500
4	429.2	36.45	0	600.5
5	535.5	51.95	0	715.0
6	646.0	44.85	0	804.5
7	752.8	46.6	0	899.5
8	867.9	19.5	0	1,007

* The values at this station are those for the rigid wing used in the lateral bending analysis. The mass moment of inertia is that for rigid wing yawing about axis through the wing elastic axis and fuselage \bar{c} .

** Positive for mass center of gravity below fuselage \bar{c} .

TABLE III

MASS DISTRIBUTION OF WING AND FUSELAGE
 (TOTAL WEIGHT 12,330 LBS.)

Wing Mass Distribution (per slice, incl. ailer.)

Wing Sta.	Dist. to Fuselage (in.)	Mass (slugs)	Mass Balance* (slug ft.)	Mass Mom. of Inertia about Elastic Axis (slug ft. ²)	Wing Strip Width (in.)
1	170.78	4.100	2.1012	0.000	104.97
2	467.26	7.886	3.329	20.10	104.97
3	338.32	17.374	10.004	0.00	121.36
4	223.04	12.324	7.2017	75.74	80.71
5	166.52	6.000	-500.05	0.000	36.0
6	132.73	8.100	-500.17	0.000	36.0
7	95.00	20.350	10.190	133.0	20.53

*Positive for mass center of gravity aft of wing elastic axis.

Aileron Mass Distribution (per side)

Aileron Sta.	Dist. to Fuselage (in.)	Mass (slugs)	Mass Balance (slug ft.)	Mass Mom. of Inertia about Elastic Axis (slug ft. ²)	Wing Strip Width (in.)
1'	522.5	2.64	0	0.625	**

**Wing strip widths for stations 1 and 2 are used for the aerodynamic loading computations.

Fuselage Mass Distribution (per slice, incl. tail surfaces)

Fuselage Sta.	Dist. aft of Nose (in.)	Mass (slugs)	Mass Balance (slug ft.)
1	71.00	32.01	0
2	133.32	33.40	0
3	181.24	31.00	0
4	223.04	21.00	0
5	266.52	21.00	0
6	312.73	17.00	0
7	361.00	21.00	0
8	411.00	11.00	0

FIGURE 3

WING STRENGTH MOMENTS

— J. Torsion
- - - I Bending

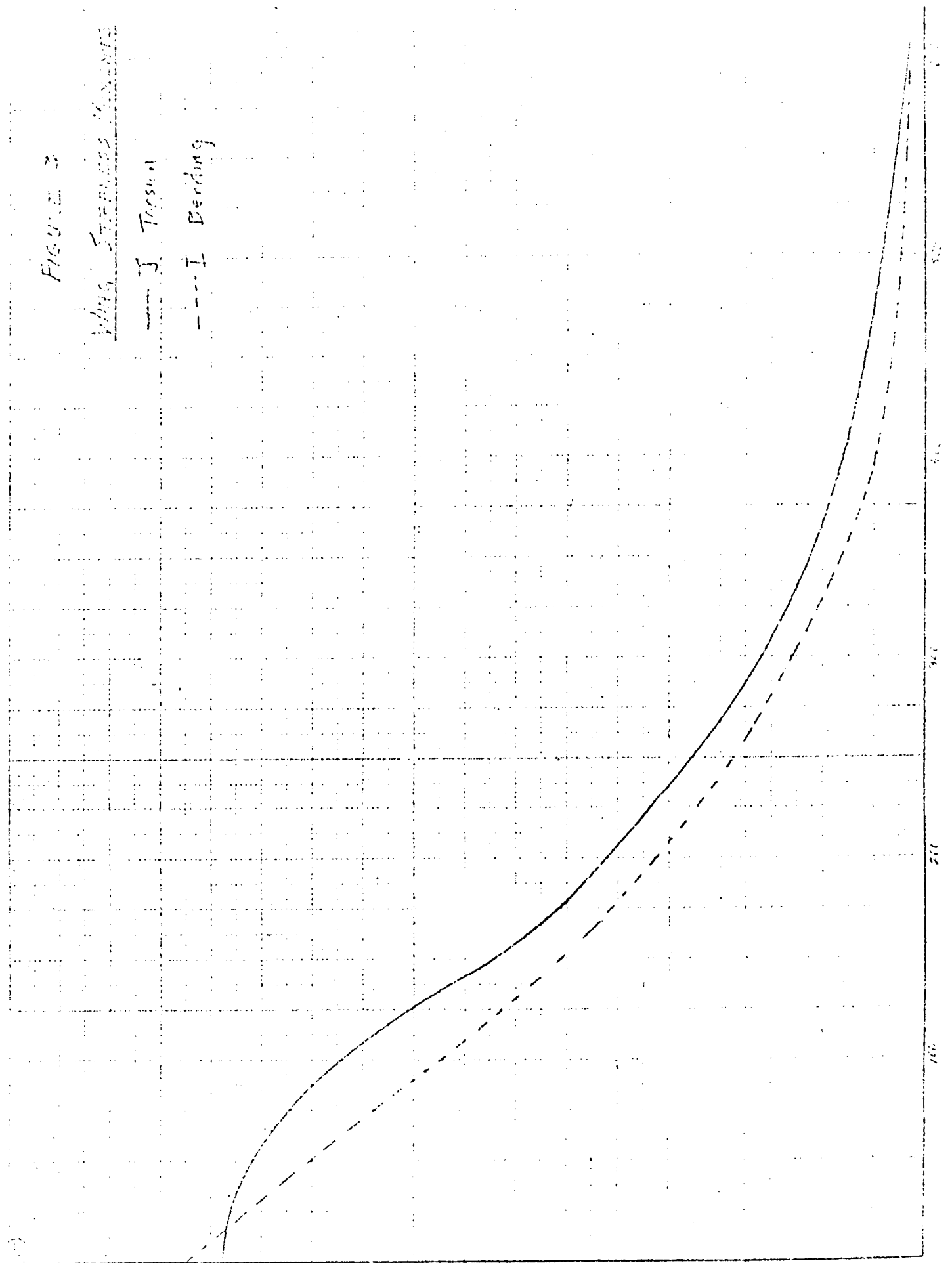


FIGURE 6
EFFECT OF STIFFNESS MOMENTS

--- J Taper
--- I Bending

Vertical end of

Code bending

Wing elastic axis

Equilibrium position

Dist. from

2000
2200
2400
2600
2800
3000
3200
3400
3600
3800
4000

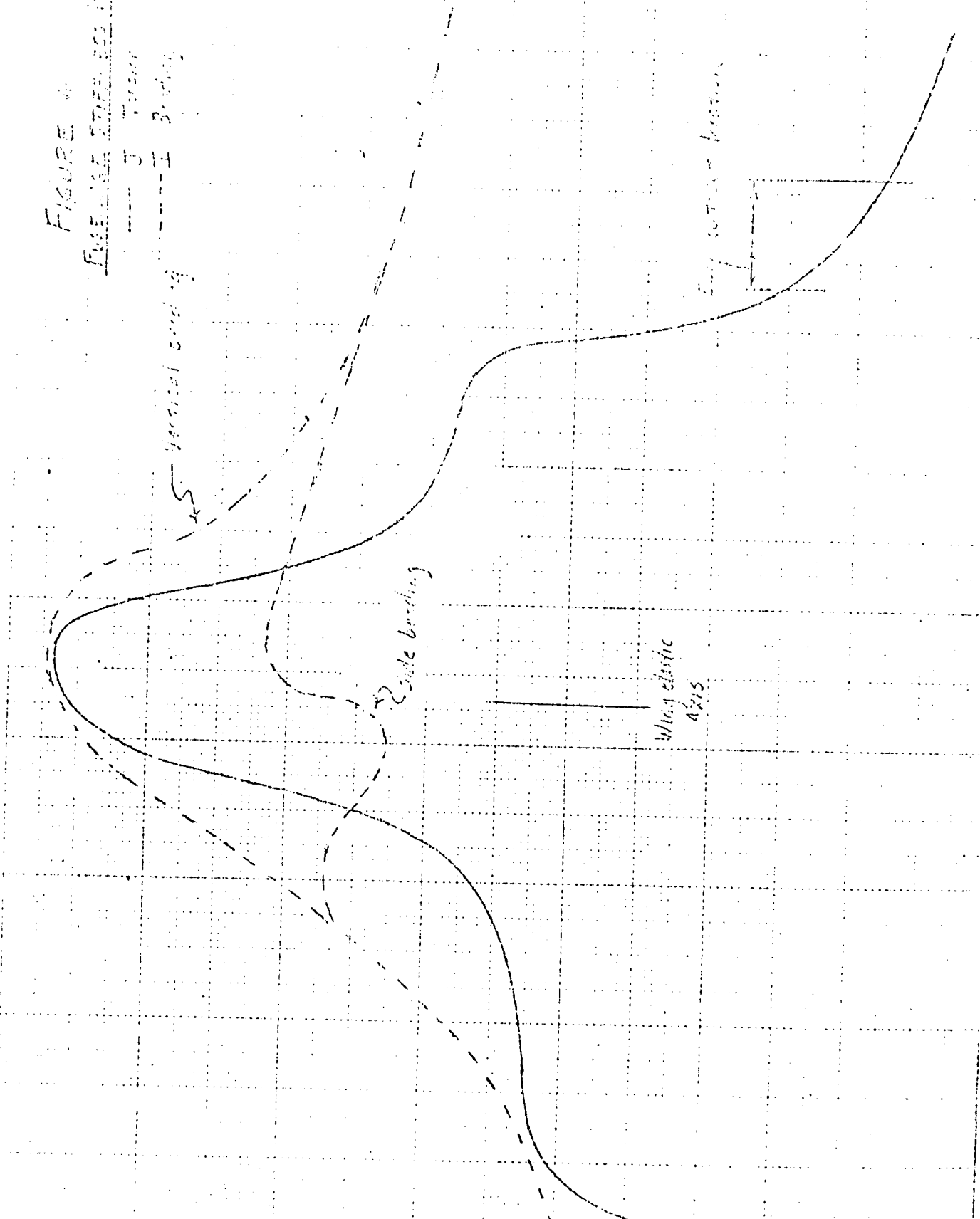


TABLE III

WING AND FUSELAGE ELASTIC COEFFICIENTS

Table III. Elastic Coefficients

Wing Sta.	Dist. aft. nose (in.)	$v_f (10^6)$ $=v_{ff} (10^6)$ rad/lb	$v_m (10^6)$ rad/in.-lb	$d_f (10^6)$ in/lb	$v_t (10^6)$ rad/lb.-lb
1	71.0	.00027	.000215	377.75	.0002117
2	133.32	1.41E-05	.000215	111.5	.0002117
3	203.24	.00027	.000714	27.047	.0002117
4	287.04	.00027	.001403	1.7177	.0002117
5	165.33	.016729	.00000003	.40093	.0002117
6	422.9	.00027	.0011326	2.2331	.0002117
7	535.5	.00027	.00000009	.70336	.0002117

Fuselage Elastic Coefficients (total)*

Fuse. Sta.	Dist. aft of fuse.nose (in.)	$v_f \times 10^6$ $=d_{ff} \times 10^6$ (rad/lb)	$v_m \times 10^6$ (rad/in. lb)	$d_f \times 10^6$ (in/lb)	$v_t \times 10^6$ (rad/in. lb)
Lateral bending					Torsion
1	71.1	.015363	.00055254	.84215	.00055440
2	133.5	.050465	.00080889	4.31701	.00095654
3	209.3	.037347	.00067183	2.52810	.00054043
4	422.9	.0073100	.00027612	.25646	.00017564
5	535.5	.022427	.00057307	2.7909	.00054774
6	656.0	.042110	.00070029	2.8402	.00064913
7	759.8	.033783	.00065068	1.76001	.0002097
8	867.9	.035588	.00072841	1.789e2	.0000746
Vertical bending					Torsion
1	71.0-5	.015448	.00050282	.64535	.0004000
2	133.32	.062954	.00070666	6.5449	.00011550
3	203.24	.013763	.00040695	1.1072	.0004130
4	422.94	.001170	.00020132	.17147	.00012004
5	535.50	.023400	.00046643	1.8092	.00054774
6	655.95	.039476	.00067254	3.0405	.000413
7	755.12	.009113	.00010001	2.0734	.0000676
8	867.9	.000032	.00017375	2.5024	.0000375

* Coefficients are listed for fuselage as two cantilever beams, each extending from 3/4" aft of nose to nose and to tail.

Figure 5.
 Location of masses and
 Elastic Axis of Tail Surfaces.

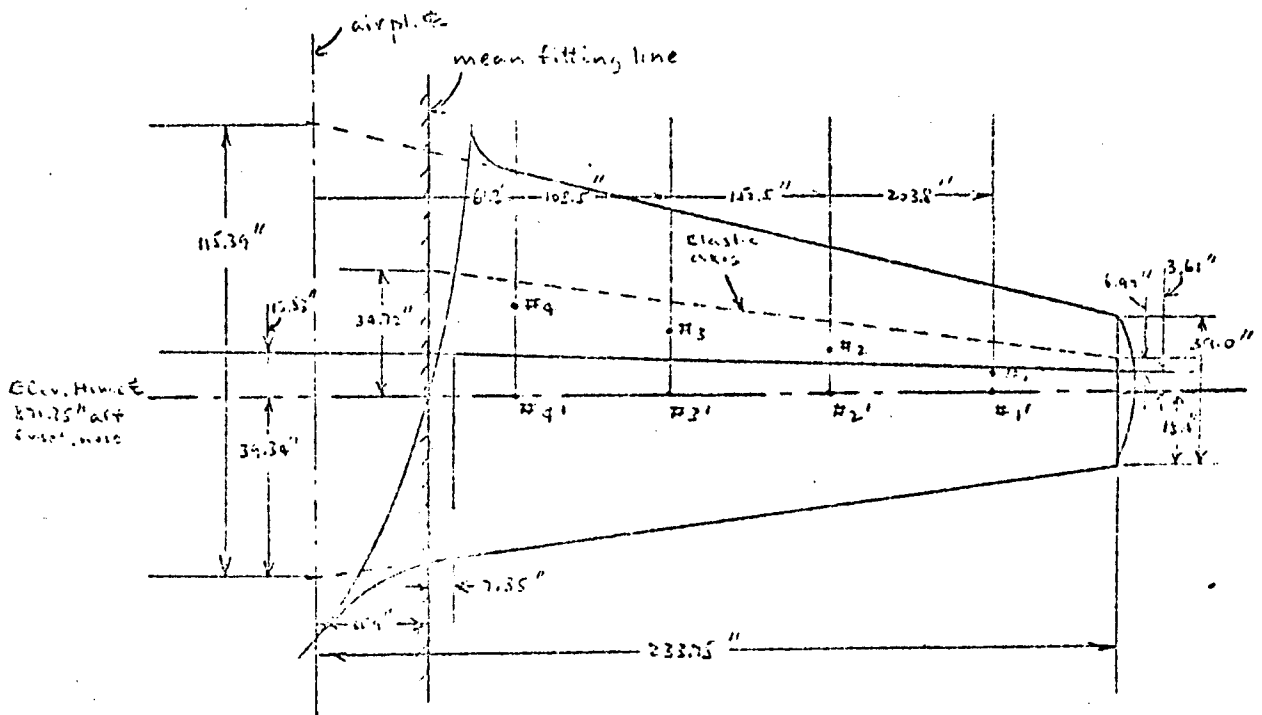
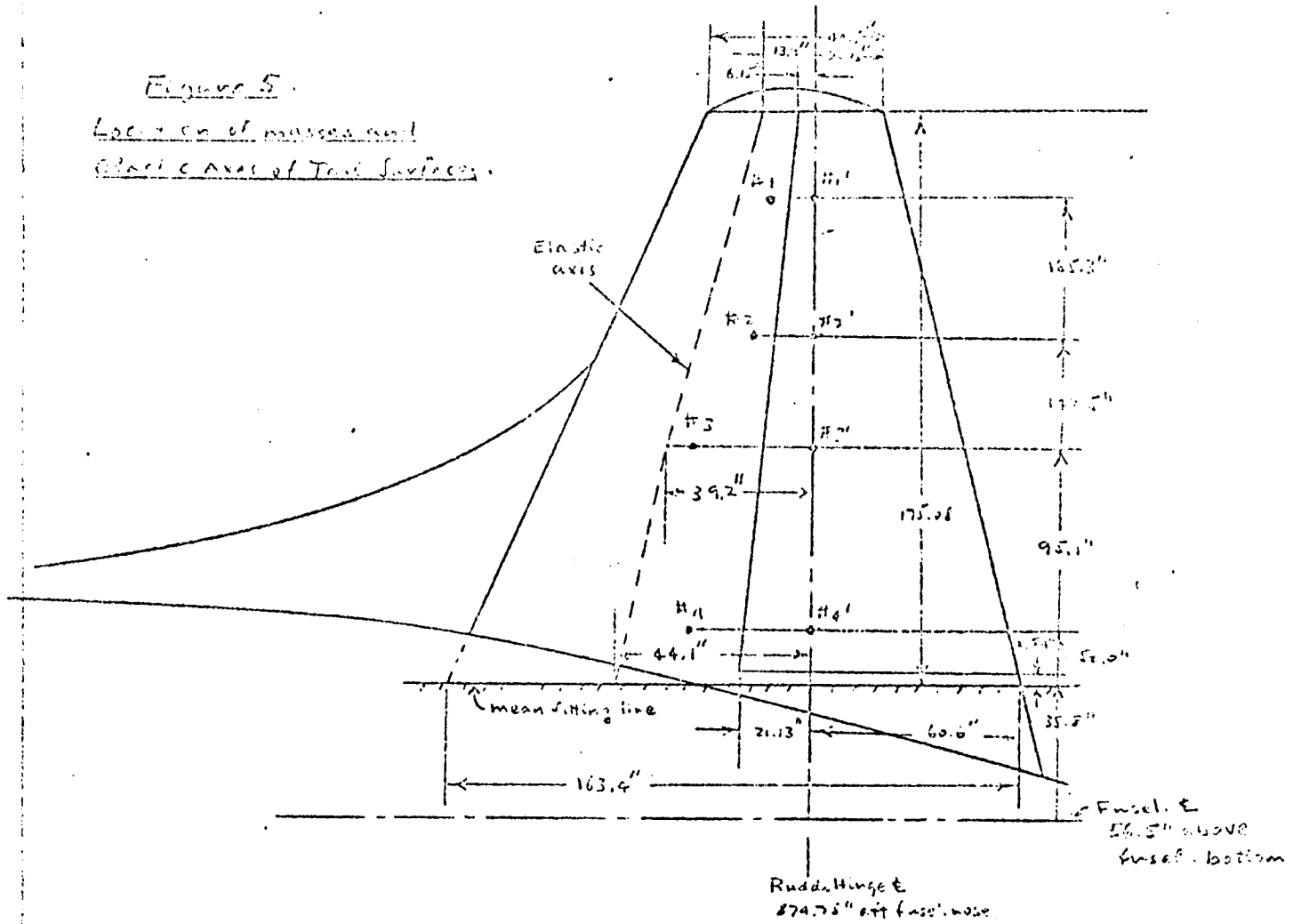


TABLE IV
 TAIL MASS DISTRIBUTION

Horizontal Stabilizer Mass Distribution (per side, incl. elev.)

Stab. Sta.	Dist. to Root (in.)	Mass (slug)	Mass Unbalance* (slug ft.)	Mass Mom. of Inertia about Elastic Axis (slug ft. ²)	Stab. Width (in.)
1	203.6	2.094	1.367	2.19	37.4
2	152.5	2.303	1.427	4.40	44.0
3	106.5	3.041	1.703	9.11	44.0
4	61.2	4.15	1.87	17.11	50.7

Elevator Mass Distribution (per side)

Elev. Sta.	Dist. to Fusel. (in.)	Mass (slug)	Mass Unbalance* (slug ft.)	Mass Mom. of Inertia about \bar{y} (slug ft. ²)	Strip Width (in.)
1'	203.6	.835	0	.3954	5.4
2'	152.5	.451	0	.5104	44.0
3'	106.5	1.227	0	1.405	44.0
4'	61.2	2.527	0	2.693	45.0

Vertical Fin (total, incl. rudder).

Fin Sta.	Dist. above Fusel. Bottom (in.)	Mass (slug)	Mass Unbalance* (slug ft.)	Mass Mom. of Inertia about Elastic axis (slug ft. ²)	Fin Width (in.)
1	241.77	1.261	1.701	3.285	4.0
2	195.04	2.273	3.026	8.31	4.0
3	151.64	5.66	4.09	62.1	3.0
4	108.47	3.568	6.95	35.03	3.0

TABLE IV (Cont'd)

Rudder Mass Distribution (Total)

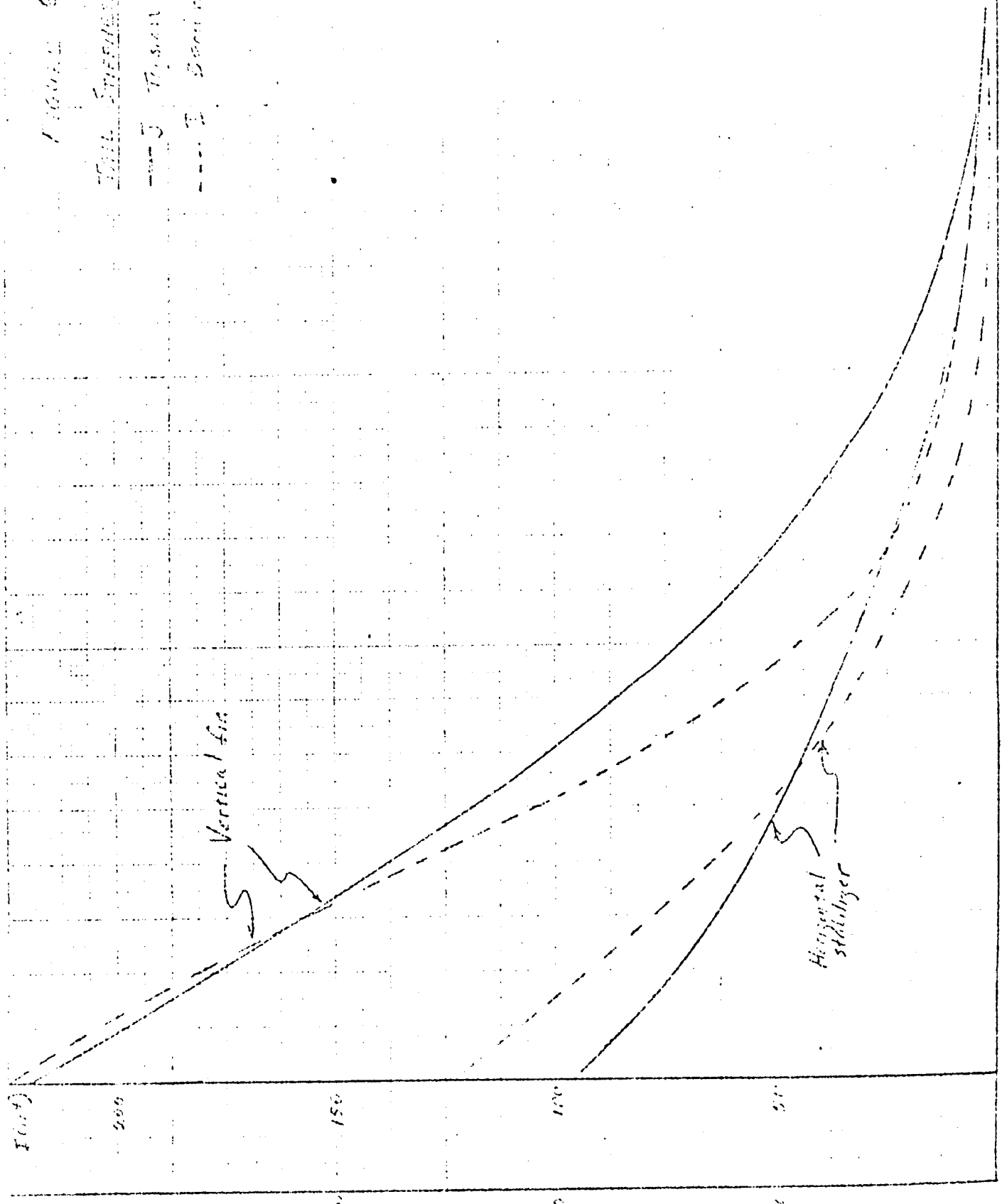
Stn. Sta.	Dist. above In. c. bottom (in.)	Mass (slugs)	Mass balance* (slug-ft.)	Mass Moment of Inertia about H (slug-ft. ²)	Strip width (in.)
1'	241.77	.836	0	.4498	47.54
2'	199.04	.979	0	.7101	40.0
3'	151.64	1.727	0	2.337	54.55
4'	108.47	1.270	0	2.629	30.1

*Positive for mass center of gravity aft of elastic axis or hinge line.

Figure 6

Tail Surface Moments

--- J. Dixon
- - - E. Boeing



Vertical fin

Horizontal stabilizer

Horizontal Stabilizer Elastic Coefficients (per side)

Stabilizer Sta.	Dist. to Airplane (in.)	$v_F(10^6)$ $=v_B(10^6)$ rad/lb	$v_H(10^6)$ rad/in-lb	$d_F(10^6)$ in/lb	$v_T(10^6)$ rad/in-lb
1	203.0	2.7100	1.3100	530.51	.01700
2	132.5	1.3100	.20722	100.00	.02700
3	103.5	1.3100	.00515	10.00	.12700
4	61.2	.2100	.02000	4.00	.04700

Vertical Fin Elastic Coefficients

Fin Sta.	Dist. above Fuselage (in.)	$v_F(10^6)$ $=v_B(10^6)$ rad/lb	$v_H(10^6)$ rad/in-lb	$d_F(10^6)$ in/lb	$v_T(10^6)$ rad/in-lb
1	241.77	2.4700	.32602	158.54	.32234
2	191.04	2.3200	.13547	67.00	.01337
3	151.04	.07900	.034381	16.7711	.00018
4	100.47	.010200	.007759	.70000	.010571

Note: Elastic coefficients as defined in Reference 1.

Calculation of Vibration Modes

The coupled bending-torsion vibrations were computed by the method described in Reference 2, modified to include flexibility of the fuselage as experienced in flight (see 3). The motions involved in an coupled mode are as follows:

1. Symmetric wing modes.
Vertical translation and rotation about the elastic axis of the wing masses, and vertical translation of fuselage masses with rigid tail surfaces.
2. Anti-symmetric wing modes.
Vertical translation and rotation about the elastic axis of the wing masses, and rotation of rigid tail and tail surfaces about the airplane longitudinal axis.
3. Lateral fuselage modes.
Lateral translation and rotation about the fuselage elastic axis of the fuselage masses and rigid tail and wing surfaces, rigid wing rotation about the airplane yaw axis, and vertical translation and rotation about the wing elastic axis of the wing masses.
4. Cantilevered tail surface modes.
Vertical translation and rotation about stabilizer elastic axis of the stabilizer masses.

The first and second coupled normal modes were computed for each of the above motions. Table VI presents the first and fuselage deflection at each station for the symmetric and anti-symmetric wing modes, based on the distribution of masses for the minimum gross weight condition. These data were applied to the maximum gross weight condition with mass coupling between the first and second modes, since the modes are orthogonal only for the minimum gross weight condition. It is noted that a factor R_H has been included in the potential energy term (involving frequencies). This correction factor is applied since the generalized mass for the maximum gross weight condition has increased above that for the minimum gross weight condition, whereas the generalized spring rate is unchanged.

Table VII presents the wing and fuselage deflections at each station for the first and second coupled lateral fuselage modes.

Table VIII presents the deflections of the vertical tail and cantilevered tail and stabilizer for the first and second coupled cantilevered modes of rigid tail surfaces.

Calculation of Vibration Index (Cv)

The principal rotational frequencies of the control surface (wing, elevator, and rudder) were assumed to be equal to zero.

TABLE VI

PREDOMINANTLY WING VIBRATIONS AND DEFLECTIONS OF BRUNNEN A-10 AIRCRAFT
 (Minimum gross weight 28,630 lbs.)

Symmetric Modes

		First Coupled Mode 20.0 rad/sec		Second Coupled Mode 30.0 rad/sec	
Wing Sta. #	Distance to Airplane ξ (in.)	f_n	f_{α} (rad/in)	f_n	f_{α} (rad/in)
1	570.8	1.0	.0003999	1.0	.01716
2	467.3	.9977	.0003012	.9979	.01676
3	336.3	.9460	.0001887	.9187	.01011
4	223.0	.00749	.0001214	.073824	.01971
5	168.5	.01446	.0001019	.1130	.01337
6	132.5	-.01093	.0009418	.3408	.003214
7	55.0	-.04308	.00005704		
Fusel. Sta. #	Distance Aft Nose (in.)	f_n^{**}		f_n^{**}	
1	71.1	-.07809		1.077	
2	133.3	-.07050		1.211	
3	283.2	-.05503		.9385	
4	429.9	-.04621		.8096	
5	535.5	-.03001		.6890	
6	656.0	-.02757		.6450	
7	753.1	-.06648		.2148	
8	867.9	-.07611		.2768	

* Positive fuselage f_n is translation of mass upward.

TABLE VI (Cont'd)

Anti-symmetric Modes**

Wing Station	Distance to Airplane \bar{x} (in.)	72.4 rad/sec		48.0 rad/sec	
		f_n	f_{α} (rad/in)	f_n	f_{α} (rad/in)
1	570.5	1.0	.002732	1.0	-.004100
2	487.3	-.2787	.002125	-.0171	-.005117
3	356.3	.01777	.002347	-.0210	-.007123
4	235.0	-.0470	.002700	-.0287	-.009129
5	168.5	-.0777	.002101	-.0308	-.008229
6	132.5	-.0934	.001797	-.0340	-.006310
7	95.0	-.0989	.000649	-.0372	-.001406

** Fuselage assumed rigid in roll for the anti-symmetric modes
 $(\frac{df_n}{dx})_F = .0005255$ rad/in = slope of wing bending curve at fuselage centerline for first coupled mode.
 $(\frac{df_n}{dx})_F = .0021319$ rad/in = slope of wing bending curve at fuselage centerline for second coupled mode.

TABLE VII
PRIME FUSELAGE FUSELAGE LATERAL VIBRATION MODE DEFLECTIONS
AND PHASES

(Maximum Gross Weight Condition for Fuselage only)

		First Coupled Mode 37.0 rad/sec		Second Coupled Mode 57.0 rad/sec	
Fuselage Sta. #	Distance Aft Nose (in)	f_h^{**}	f_α^{**} (rad/in)	f_h^{**}	f_α^{**} (rad/in)
1	71.1	.4446	.0004506	-.1407	.0721
2	133.7	.2749	.0004490	-.6510	.0722
3	200.3	-.0241	.0004386	-.1408	.0723
4	421.9	-.2401	.0004370	-.2118	.0724
5	533.5	-.1107	.0004739	-.5111	.0725
6	656.0	.1701	.0005248	-.09406	-.01707
7	759.8	.5491	.0006401	1.0732	-.1271
8	867.9	1.0	.0008617	1.0	-.3506

Wing Sta. #	Distance to Airplane (in)	f_h	f_α (rad/in)	f_h	f_α (rad/in)
1	570.6	-.1157	.001461	-33.17	.1560
2	467.3	-.02137	.001471	-.619	.1511
3	338.3	.004094	.001465	+14.93	.1443
4	223.0	.02143	.001430	+13.115	.1410
5	160.5	.02109	.001414	+10.30	.1362
6	132.5	.02124	.001241	+8.00	.1101
7	55.0	.01159	.0004067	+3.436	.04103

$f_{h1}^{**} = .92$ $f_{\alpha1}^{**} \approx f_{\alpha2}^{**} = \frac{0.00147}{0.00147} = 1.0$ $f_{h2}^{**} = .47$ $f_{\alpha2}^{**} \approx f_{\alpha1}^{**} = -\frac{35}{1.0} = -35$
 $\left(\frac{df_h^{**}}{dx}\right)_{x=0} = \frac{0.0119}{0.00147}$ $\left(\frac{df_\alpha^{**}}{dx}\right)_{x=0} = \frac{0.00422}{0.00147}$ $\left(\frac{df_h^{**}}{dx}\right)_{x=0} = \frac{0.116}{0.00147}$ $\left(\frac{df_\alpha^{**}}{dx}\right)_{x=0} = \frac{0.02093}{0.00147}$

* Positive fuselage f_h is translation of mass to right.

** Positive fuselage f_α is roll of mass to right.

TABLE VIII

CANTILEVERED WALL SPACE REFLECTION SHAPES AND PROPERTIES

Horizontal Stabilizer Modes

		First Coupled Mode		Second Coupled Mode	
Stab. #	Dist. to Aft. Edge (in)	35.5 Fin. Sec.		141.0 Fin. Sec.	
		f_n	$f_a \frac{rad}{in}$	f_n	$f_a \frac{rad}{in}$
1	203.8	1.0	.002307	1.0	-.03167
2	152.1	.4421	.001337	-.7716	-.03061
3	100.5	.1658	.0006697	-.5685	-.02361
4	51.2	.0775	.0001793	-.07348	-.007216

Vertical Fin Modes

		First Coupled Mode		Second Coupled Mode	
Fin Sta. #	Dist. Above Fusel. Bottom (in)	66.5 Fin. Sec.		144 Fin. Sec.	
		f_n	$f_a \frac{rad}{in}$	f_n	$f_a \frac{rad}{in}$
1	241.77	1.0	.00346	1.0	-.02415
2	199.04	.47512	.00153	.05303	-.02076
3	151.04	.1492	.000368	-.1480	-.02536
4	108.49	.0435	.0000	-.01799	-.007234

Flutter Analysis

The flutter analysis of the 13 conditions described in the Introduction were made by the method of Reference 1 and are based on the coupled modes of the Gate Inlet of Vibration Modes section. Briefly, the Lagrangian equation of motion was applied to the flutter modes considered for each condition analyzed, and the resulting equations of motion solved by means of determinants to determine the damping coefficients γ versus speed variations. The determinant solved was of the form:

$$\begin{vmatrix} A_{11} & A_{12} & A_{13} \\ A_{21} & A_{22} & A_{23} \\ A_{31} & A_{32} & A_{33} \end{vmatrix} = 0$$

It is to be noted that conditions 2, 4, 6, 8, 11, and 13 are binary cases wherein Determinant elements A_{13} , A_{23} , A_{31} , A_{32} , and A_{33} are equal to zero.

The expressions for the determinant elements are presented in Table IX for each flutter condition. The results of the critical root for each of the 13 conditions are presented in figures 7 to 13 as damping versus speed curves. It is to be noted that the speed coordinate of these curves is uncorrected for compressibility.

TABLE IX

STABILITY DETERMINANT ELEMENTS

COND. 1 Maximum Gross Weight (75,200 lbs)
Symmetric first coupled wing mode (22.7 rad/sec.) -
Symmetric second coupled wing mode (36.3 rad/sec.) -
roll rotation (0 rad/sec.)

$$A_{11} = \left[1 - \left(\frac{U_0}{V_0} \right)^2 R_F \Omega^2 \right] \left[\sum_w (M_w f_h^{(1)2} + 2 S_w f_h^{(1)} f_x^{(1)} + I_w f_x^{(1)2}) + \sum_F \frac{I_F}{F} \left(\frac{f_h^{(1)}}{b} \right)^2 + \sum_F M_F f_{hF}^{(1)2} \right] + \pi F \left[\int_w b^2 f_h^{(1)2} dx - 2a \int_w b^3 f_h^{(1)} f_x^{(1)} dx + \left(\frac{1}{2} + a^2 \right) \int_w b^4 f_x^{(1)2} dx + L_{h_1} b_r \left(\int_w b \{ f_h^{(1)2} - \left(\frac{1}{2} + a \right) 2b f_h^{(1)} f_x^{(1)} + \left(\frac{1}{2} + a \right)^2 b^2 f_x^{(1)2} \} dx \right) + L_{\alpha_1} b_r \left(\int_w b^2 \{ f_h^{(1)} - \left(\frac{1}{2} + a \right) b f_x^{(1)} \} f_x^{(1)} dx \right) + L_{\alpha_2} b_r^2 \left(\int_w b \{ f_h^{(1)} - \left(\frac{1}{2} + a \right) b f_x^{(1)} \} f_x^{(1)} dx \right) + M_{\alpha_1} b_r \int_w b^3 f_x^{(1)2} dx \right]$$

$$A_{12} = \sum_w (M_w f_h^{(1)} f_h^{(2)} + S_w \{ f_h^{(1)} f_x^{(2)} + f_h^{(2)} f_x^{(1)} \} + I_w f_x^{(1)} f_x^{(2)}) + \sum_F \frac{I_F}{F} f_{hF}^{(1)} f_{hF}^{(2)} + \sum_F \frac{I_F}{F} f_{hF}^{(1)2} + \pi F \left[\int_w b^2 f_h^{(1)} f_h^{(2)} dx - a \left(\int_w b^3 \{ f_h^{(1)} f_x^{(2)} + f_h^{(2)} f_x^{(1)} \} dx \right) + \left(\frac{1}{2} + a^2 \right) \int_w b^4 f_x^{(1)} f_x^{(2)} dx + L_{h_1} b_r \left(\int_w b \{ f_h^{(1)} f_h^{(2)} - \left(\frac{1}{2} + a \right) b \{ f_h^{(1)} f_x^{(2)} + f_h^{(2)} f_x^{(1)} \} + \left(\frac{1}{2} + a \right)^2 b^2 f_x^{(1)} f_x^{(2)} \} dx \right) + L_{\alpha_1} b_r \left(\int_w b^2 \{ f_h^{(1)} - \left(\frac{1}{2} + a \right) b f_x^{(1)} \} f_x^{(2)} dx \right) + L_{\alpha_2} b_r^2 \left(\int_w b \{ f_h^{(1)} - \left(\frac{1}{2} + a \right) b f_x^{(1)} \} f_x^{(2)} dx \right) + M_{\alpha_1} b_r \left(\int_w b^3 f_x^{(1)} f_x^{(2)} dx \right) \right]$$

$$A_{21} = \sum_w (M_w f_h^{(2)} f_h^{(1)} + S_w \{ f_h^{(2)} f_x^{(1)} + f_h^{(1)} f_x^{(2)} \} + I_w f_x^{(2)} f_x^{(1)}) + \sum_F \frac{I_F}{F} f_{hF}^{(2)} f_{hF}^{(1)} + \sum_F \frac{I_F}{F} f_{hF}^{(2)2} + \pi F \left[\int_w b^2 f_h^{(2)} f_h^{(1)} dx - a \left(\int_w b^3 \{ f_h^{(2)} f_x^{(1)} + f_h^{(1)} f_x^{(2)} \} dx \right) + \left(\frac{1}{2} + a^2 \right) \int_w b^4 f_x^{(2)} f_x^{(1)} dx + L_{h_1} b_r \left(\int_w b \{ f_h^{(2)} f_h^{(1)} - \left(\frac{1}{2} + a \right) b \{ f_h^{(2)} f_x^{(1)} + f_h^{(1)} f_x^{(2)} \} + \left(\frac{1}{2} + a \right)^2 b^2 f_x^{(2)} f_x^{(1)} \} dx \right) + L_{\alpha_1} b_r \left(\int_w b^2 \{ f_h^{(2)} - \left(\frac{1}{2} + a \right) b f_x^{(2)} \} f_x^{(1)} dx \right) + L_{\alpha_2} b_r^2 \left(\int_w b \{ f_h^{(2)} - \left(\frac{1}{2} + a \right) b f_x^{(2)} \} f_x^{(1)} dx \right) + M_{\alpha_1} b_r \left(\int_w b^3 f_x^{(2)} f_x^{(1)} dx \right) \right]$$

TABLE IX - Cont'd.

$$\begin{aligned}
 A_{22} = & [1 - R_2 \Omega] \left[\sum_w (M_w f_h^{(10)} + 2 S_w f_h^{(10)} f_x^{(10)} + I_w f_x^{(10)}) + \sum_F M_f f_{hf}^{(10)} + \sum_F I_f \right. \\
 & + \pi \rho \left[\int_w b^2 f_h^{(10)2} dx - 2a \int_w b^3 f_h^{(10)} f_x^{(10)} dx + \left(\frac{1}{2} + a^2\right) \int_w b^4 f_x^{(10)2} dx \right. \\
 & \left. + L_{h_1} b_r \left(\int_w b \left\{ f_h^{(10)2} - (1/2 + a) 2b f_h^{(10)} f_x^{(10)} + (1/2 + a)^2 b^2 f_x^{(10)2} \right\} dx \right) \right. \\
 & \left. + L_{h_2} b_r \left(\int_w b^2 \left\{ f_h^{(10)} - (1/2 + a) b f_x^{(10)} \right\} f_x^{(10)} dx + L_{x_2} b_r^2 \left(\int_w b \left\{ f_h^{(10)} - (1/2 + a) b f_x^{(10)} \right\} f_x^{(10)} \right. \right. \right. \\
 & \left. \left. \left. + M_{x_1} b_1 \int_w b^3 f_x^{(10)2} dx \right) \right]
 \end{aligned}$$

$$\begin{aligned}
 A_{13} = & I_A f_{x_A}^{(11)} + \pi \rho \left[\left\{ L_\beta - (c-e) L_z \right\} \int_A b^3 f_h^{(11)} dx + \left\{ M_\beta - (1/2 + a) L_\beta \right. \right. \\
 & \left. \left. - (c-e) M_z + (1/2 + a)(c-e) L_z \right\} \int_A b^4 f_x^{(11)} dx \right]
 \end{aligned}$$

$$\begin{aligned}
 A_{23} = & I_A f_{x_A}^{(12)} + \pi \rho \left[\left\{ L_\beta - (c-e) L_z \right\} \int_A b^3 f_h^{(12)} dx + \left\{ M_\beta - (1/2 + a) L_\beta \right. \right. \\
 & \left. \left. - (c-e) M_z + (1/2 + a)(c-e) L_z \right\} \int_A b^4 f_x^{(12)} dx \right]
 \end{aligned}$$

$$\begin{aligned}
 A_{31} = & I_A f_{x_A}^{(11)} + \pi \rho \left[\left\{ T_h - (c-e) P_h \right\} \int_A b^3 f_h^{(11)} dx + \left\{ T_x - (1/2 + a) T_h \right. \right. \\
 & \left. \left. - (c-e) P_x + (1/2 + a)(c-e) P_h \right\} \int_A b^4 f_x^{(11)} dx \right]
 \end{aligned}$$

$$\begin{aligned}
 A_{32} = & I_A f_{x_A}^{(12)} + \pi \rho \left[\left\{ T_h - (c-e) P_h \right\} \int_A b^3 f_h^{(12)} dx + \left\{ T_x - (1/2 + a) T_h \right. \right. \\
 & \left. \left. - (c-e) P_x + (1/2 + a)(c-e) P_h \right\} \int_A b^4 f_x^{(12)} dx \right]
 \end{aligned}$$

$$A_{33} = I_A + \pi \rho \left[T_\beta - (c-e)(P_\beta + T_z) + (c-e)^2 P_z \right] \int_A b^4 dx$$

note: $\left(\frac{df_h^{(11)}}{dx} \right)_F, \left(\frac{df_h^{(12)}}{dx} \right)_F = 0$

TABLE II (Cont'd.)

Notation:

- M_w = mass of the wing stations (TABLE I)
- S_w = mass unbalance of the wing stations (TABLE I)
- I_w = mass moment of inertia of the wing stations (TABLE I)
- I_f = mass moment of inertia of the fuselage stations (TABLE I)
- M_F = mass of the fuselage stations (TABLE I)
- I_n = mass moment of inertia of the airfoil (TABLE I)
- $f_n^{(1)}, f_n^{(2)}$ = wing bending deflection shapes of the symmetric first and second coupled wing modes respectively (TABLE VI)
- $f_x^{(1)}, f_x^{(2)}$ = wing torsion deflection shapes of the symmetric first and second coupled wing modes respectively (TABLE VI)
- $f_{nf}^{(1)}, f_{nf}^{(2)}$ = fuselage bending deflection shapes of the symmetric first and second coupled wing modes respectively (TABLE VI)
- $\left(\frac{df_n^{(1)}}{dx}\right)_{x=0}, \left(\frac{df_n^{(2)}}{dx}\right)_{x=0}$ = slopes of wing bending curves at the fuselage centerline for the first and second antisymmetric coupled wing modes respectively (TABLE III)
- $f_{tn}^{(1)}, f_{tn}^{(2)}$ = wing torsional displacements at the airfoil section for the first and second symmetric coupled wing modes respectively

TABLE IX - Cont'd.

u_1, u_2 = frequencies for the first and second coupled modes respectively with the values given in the conditions.

R_1, R_2 = ratios of the values of the generalized mass for the minimum gross weight condition to that for the maximum gross weight condition for the first and second coupled modes respectively, i.e.

$$R_1 = \frac{\left[\sum_{n=1}^2 (M_w f_n^{(m)^2} + 2 S_w f_h^{(m)} f_n^{(m)} + I_w f_n^{(m)^2}) + \sum_{F=1}^2 M_F f_{hF}^{(m)^2} \right]^*}{\left[\sum_{n=1}^2 (M_w f_n^{(M)^2} + 2 S_w f_h^{(M)} f_n^{(M)} + I_w f_n^{(M)^2}) + \sum_{F=1}^2 M_F f_{hF}^{(M)^2} \right]**}$$

* minimum gross weight values for M_w, S_w, I_w, M_F from TABLE II

** maximum gross weight values for M_w, S_w, I_w, M_F from TABLE I

b_r = wing reference semi-chord = 3.26 ft

ρ = density of air at 10,000 ft. altitude = $.001752 \frac{lb-cu}{ft^3}$

c = airfoil hinge loc. = .58

c = " lead edge " = 0

$L_{h1}, L_{\alpha 1}, M_{\alpha 1}$ = $L_{h2}, L_{\alpha 2}, M_{\alpha 2}$ coeff. components depend. on $\frac{v}{b \omega}$

$L_{\alpha 2}$ = $L_{\alpha 2}$ coeff. component depend. on $\left(\frac{v}{b \omega}\right)^2$

(cont.)

TABLE IX - Cont'd.

COND. 2 Maximum Gross Weight (53,200 lbs.)

Symmetric first coupled wing mode (22.9 rad/sec.) -
symmetric second coupled wing mode (36.8 rad/sec.)

$A_{11}, A_{12}, A_{21}, A_{22} =$ same as for condition 1

$A_{13}, A_{23}, A_{31}, A_{32}, A_{33} = 0$ (four elements in determinant)

COND. 3 Maximum Gross Weight (53,200 lbs.)

Antisymmetric first coupled wing mode (29.8 rad/sec.)
antisymmetric second coupled wing mode (48.0 rad/sec.)
aileron rotation (0 rad/sec.)

$A_{11}, A_{12}, A_{21}, A_{22} =$ same as for condition 1 using
deflection shapes for antisymmetric modes (TABLE V)
 $f_{hF}^{(1)}, f_{hF}^{(2)} = 0$; $(\frac{df_h^{(1)}}{dx})_2, (\frac{df_h^{(2)}}{dx})_2 \neq 0$ (TABLE VI); \bar{F}_1, \bar{F}_2
values for the antisymmetric modes; \bar{I}_1 values (TABLE

$A_{13}, A_{23}, A_{31}, A_{32}, A_{33} =$ same as for condition 1 using
values of $f_{dN}^{(1)}, f_{dN}^{(2)}$ for antisymmetric modes (TABLE V)

COND. 4 Maximum Gross Weight (53,200 lbs.)

Antisymmetric first coupled wing mode (29.8 rad/sec.)
antisymmetric second coupled wing mode (48.0 rad/sec.)

$A_{11}, A_{12}, A_{21}, A_{22} =$ same as for condition 3

$A_{13}, A_{23}, A_{31}, A_{32}, A_{33} = 0$ (four elements in determinant)

TABLE IX - Cont'd.

COND. 5 Minimum Gross Weight (28,630 lbs.)

Symmetric first coupled wing mode (22.9 rad/sec.) -
symmetric second coupled wing mode (36.8 rad/sec.) -
aileron rotation (0 rad/sec.)

A_{11}, A_{22} = same as for condition 1 using minimum
gross weight values for M_w, S_w, I_w, M_r (TABLE II)
 $R_1, R_2 = 1$

A_{12}, A_{21} = same as for condition 1 with
$$\left[\sum_u (M_u f_u^{(1)} f_u^{(2)}) + S_w \{ f_w^{(1)} f_w^{(2)} + f_w^{(3)} f_w^{(4)} \} + I_w (f_w^{(1)} f_w^{(2)}) + \sum_r (M_r f_r^{(1)} f_r^{(2)}) \right] = 0$$

$A_{13}, A_{23}, A_{31}, A_{32}, A_{33}$ = same as for condition 1

COND. 6 Minimum Gross Weight (28,630 lbs.)

Symmetric first coupled wing mode (22.9 rad/sec.) -
symmetric second coupled wing mode (36.8 rad/sec.)

$A_{11}, A_{12}, A_{21}, A_{22}$ = same as for condition 5

$A_{13}, A_{23}, A_{31}, A_{32}, A_{33} = 0$ (four elements in determinant)

TABLE II - Cont'd.

COND. 7 Minimum Gross Weight (28,630 lbs)
Antisymmetric first coupled wing mode (29.8 rad/sec.)
antisymmetric second coupled wing mode (46.6 rad/sec)
aileron (0 rad/sec.)

$A_{11}, A_{22} =$ same as for condition 3 using minimum gross weight values for M_w, S_w, I_w, I_F (TABLE II)
 $R_1, R_2 = 1$

$A_{12}, A_{21} =$ same as for condition 3 with
$$\left[\sum_w (M_w f_h^{(1)} f_h^{(2)} + S_w \{ f_h^{(1)} f_h^{(2)} + f_h^{(2)} f_h^{(1)} \} + I_w f_x^{(1)} f_x^{(2)}) + \sum_F I_F \frac{d f_h^{(1)}}{dx} \frac{d f_h^{(2)}}{dx} \right] =$$

$A_{13}, A_{23}, A_{31}, A_{33} =$ same as for condition 1

COND. 8 Minimum Gross Weight (28,630 lbs)
Antisymmetric first coupled wing mode (29.8 rad/sec.)
antisymmetric second coupled wing mode (46.6 rad/sec)

$A_{11}, A_{12}, A_{21}, A_{22} =$ same as for condition 7

$A_{13}, A_{23}, A_{31}, A_{32}, A_{33} = 0$ (four elements in determinant)

TABLE IX - Cont'd.

Cond. 4. Maximum Weight Fuselage, Minimum Weight Wing (G.W. 41, 52)
 Antisymmetric first coupled fuselage mode (37.0 $\frac{r_{h,d}}{r_{h,c}}$) vs.
 second coupled fuselage mode (56.0 $\frac{r_{h,d}}{r_{h,c}}$) vs. rudder rotation (0)

$$\begin{aligned}
 A_{11} = & \left[1 - \left(\frac{\omega}{\omega_2} \right)^2 \Omega^2 \right] \left[\sum_w (M_w f_h^{(1)2} + 2 S_w f_h^{(1)} f_{\alpha}^{(1)} + I_w f_{\alpha}^{(1)2}) + \sum_F (M_F f_h^{(1)2} + 2 S_F f_h^{(1)} f_{\alpha}^{(1)} + I_F f_{\alpha}^{(1)2}) + \left(\frac{d f_h^{(1)}}{d x} \right)_c^2 \sum_w M_w x^2 \right. \\
 & + \pi \rho \left[\int_f b^2 (f_{h_f}^{(1)2} + 2 x f_{h_f}^{(1)} f_{\alpha_f}^{(1)} + x^2 f_{\alpha_f}^{(1)2}) dx + \left(\frac{d f_h^{(1)}}{d x} \right)_f \int_f b^2 (f_{h_f}^{(1)} + x f_{\alpha_f}^{(1)} - \frac{2x}{l} \left(\frac{d f_h^{(1)}}{d x} \right)_f) dx + f_{\alpha_f}^{(1)2} \int_f b^2 x^2 \right. \\
 & + L_{h_1} b_r \int_f b (f_{h_f}^{(1)2} + 2 x f_{h_f}^{(1)} f_{\alpha_f}^{(1)} + x^2 f_{\alpha_f}^{(1)2}) dx + L_{h_{1.5}} b_{r_2} f_{\alpha_f}^{(1)2} \int_f b x^2 dx + L_{\alpha_1} b_r \left(\frac{d f_h^{(1)}}{d x} \right)_f \int_f b^2 x^2 dx + x f_{\alpha_f}^{(1)} \\
 & \left. \left. + L_{\alpha_2} b_r \left(\frac{d f_h^{(1)}}{d x} \right)_f \int_f b (f_{h_f}^{(1)} + x f_{\alpha_f}^{(1)}) dx + M_{\alpha_1} b_r \left(\frac{d f_h^{(1)}}{d x} \right)_f^2 \int_f b^2 dx \right] \right]
 \end{aligned}$$

$$\begin{aligned}
 A_{12} = & \pi \rho \left[\int_f b^2 (f_{h_f}^{(1)} f_{\alpha_f}^{(1)} + x (f_{h_f}^{(1)} f_{\alpha_f}^{(1)} - f_{h_{\alpha_f}}^{(1)} f_{\alpha_f}^{(1)}) + x^2 f_{\alpha_f}^{(1)} f_{\alpha_f}^{(1)}) dx + \frac{1}{2} \int_f b^2 \left(\frac{d f_h^{(1)}}{d x} \right)_c \left(f_{h_f}^{(1)} + x f_{\alpha_f}^{(1)} \right) + \left(\frac{d f_h^{(1)}}{d x} \right)_c \left(f_{h_f}^{(1)} + x \right. \right. \\
 & \left. \left. + \frac{2}{l} \left(\frac{d f_h^{(1)}}{d x} \right)_f \left(\frac{d f_h^{(1)}}{d x} \right)_c \int_f b^2 dx + f_{\alpha_f}^{(1)} f_{\alpha_f}^{(1)} \int_f b^2 x^2 dx + L_{h_1} b_r \int_f b (f_{h_f}^{(1)} f_{\alpha_f}^{(1)} + x (f_{h_f}^{(1)} f_{\alpha_f}^{(1)} + f_{h_{\alpha_f}}^{(1)} f_{\alpha_f}^{(1)}) + x^2 f_{\alpha_f}^{(1)} f_{\alpha_f}^{(1)}) \right. \right. \\
 & \left. \left. + L_{\alpha_1} b_r \left(\frac{d f_h^{(1)}}{d x} \right)_c \int_f b^2 (f_{h_f}^{(1)} + x f_{\alpha_f}^{(1)}) dx + L_{\alpha_2} b_r \left(\frac{d f_h^{(1)}}{d x} \right)_f \int_f b (f_{h_f}^{(1)} + x f_{\alpha_f}^{(1)}) dx + M_{\alpha_1} b_r \left(\frac{d f_h^{(1)}}{d x} \right)_c \left(\frac{d f_h^{(1)}}{d x} \right)_f \int_f b \right. \right. \\
 & \left. \left. + L_{h_{1.5}} b_{r_2} f_{\alpha_f}^{(1)} f_{\alpha_f}^{(1)} \int_f b x^2 dx \right]
 \end{aligned}$$

$$\begin{aligned}
 A_{21} = & \pi \rho \left[\int_f b^2 (f_{h_f}^{(1)} f_{\alpha_f}^{(1)} + x (f_{h_f}^{(1)} f_{\alpha_f}^{(1)} + f_{h_{\alpha_f}}^{(1)} f_{\alpha_f}^{(1)}) + x^2 f_{\alpha_f}^{(1)} f_{\alpha_f}^{(1)}) dx + \frac{1}{2} \int_f b^2 \left(\frac{d f_h^{(1)}}{d x} \right)_c (f_{h_f}^{(1)} + x f_{\alpha_f}^{(1)}) + \left(\frac{d f_h^{(1)}}{d x} \right)_c (f_{h_f}^{(1)} + x \right. \right. \\
 & \left. \left. + \frac{2}{l} \left(\frac{d f_h^{(1)}}{d x} \right)_f \left(\frac{d f_h^{(1)}}{d x} \right)_c \int_f b^2 dx + f_{\alpha_f}^{(1)} f_{\alpha_f}^{(1)} \int_f b^2 x^2 dx + L_{h_1} b_r \int_f b (f_{h_f}^{(1)} f_{\alpha_f}^{(1)} + x (f_{h_f}^{(1)} f_{\alpha_f}^{(1)} + f_{h_{\alpha_f}}^{(1)} f_{\alpha_f}^{(1)}) + x^2 f_{\alpha_f}^{(1)} f_{\alpha_f}^{(1)}) \right. \right. \\
 & \left. \left. + 2 L_{\alpha_1} b_r \left(\frac{d f_h^{(1)}}{d x} \right)_c \int_f b^2 (f_{h_f}^{(1)} + x f_{\alpha_f}^{(1)}) dx + L_{\alpha_2} b_r \left(\frac{d f_h^{(1)}}{d x} \right)_f \int_f b (f_{h_f}^{(1)} + x f_{\alpha_f}^{(1)}) dx + M_{\alpha_1} b_r \left(\frac{d f_h^{(1)}}{d x} \right)_c \left(\frac{d f_h^{(1)}}{d x} \right)_f \int_f b \right. \right. \\
 & \left. \left. + L_{h_{1.5}} b_{r_2} f_{\alpha_f}^{(1)} f_{\alpha_f}^{(1)} \int_f b x^2 dx \right]
 \end{aligned}$$

$$\begin{aligned}
 A_{22} = & \left[1 - \Omega^2 \right] \left[\sum_w (M_w f_h^{(2)2} + 2 S_w f_h^{(2)} f_{\alpha}^{(2)} + I_w f_{\alpha}^{(2)2}) + \sum_F (M_F f_h^{(2)2} + 2 S_F f_h^{(2)} f_{\alpha}^{(2)} + I_F f_{\alpha}^{(2)2}) + \left(\frac{d f_h^{(2)}}{d x} \right)_c^2 \sum_w M_w x^2 \right. \\
 & + \pi \rho \left[\int_f b^2 (f_{h_f}^{(2)2} + 2 x f_{h_f}^{(2)} f_{\alpha_f}^{(2)} + x^2 f_{\alpha_f}^{(2)2}) dx + f_{\alpha_f}^{(2)2} \int_f b^2 x^2 dx + \left(\frac{d f_h^{(2)}}{d x} \right)_f \int_f b^2 (f_{h_f}^{(2)} + x f_{\alpha_f}^{(2)} - \frac{2x}{l} \left(\frac{d f_h^{(2)}}{d x} \right)_f) dx \right. \\
 & + L_{h_1} b_r \int_f b (f_{h_f}^{(2)2} + 2 x f_{h_f}^{(2)} f_{\alpha_f}^{(2)} + x^2 f_{\alpha_f}^{(2)2}) dx + L_{h_{1.5}} b_{r_2} f_{\alpha_f}^{(2)2} \int_f b x^2 dx + L_{\alpha_1} b_r \left(\frac{d f_h^{(2)}}{d x} \right)_f \int_f b^2 (f_{h_f}^{(2)} + x f_{\alpha_f}^{(2)}) \\
 & \left. \left. + L_{\alpha_2} b_r \left(\frac{d f_h^{(2)}}{d x} \right)_c \int_f b (f_{h_f}^{(2)} + x f_{\alpha_f}^{(2)}) dx + M_{\alpha_1} b_r \left(\frac{d f_h^{(2)}}{d x} \right)_c^2 \int_f b^2 dx \right] \right]
 \end{aligned}$$

$$A_{13} = \pi \rho \left[(L_{\beta} - (c-a)L_2) \int_f b^2 (f_{h_f}^{(1)} + x f_{\alpha_f}^{(1)}) dx + (M_{\beta} - (c-a)M_2) \left(\frac{d f_h^{(1)}}{d x} \right)_c \int_f b^2 dx \right] + \left(\frac{d f_h^{(1)}}{d x} \right)_c \int_f \frac{1}{l} dx$$

$$A_{23} = \pi \rho \left[(L_{\beta} - (c-a)L_2) \int_f b^2 (f_{h_f}^{(2)} + x f_{\alpha_f}^{(2)}) dx + (M_{\beta} - (c-a)M_2) \left(\frac{d f_h^{(2)}}{d x} \right)_c \int_f b^2 dx \right] + \left(\frac{d f_h^{(2)}}{d x} \right)_c \int_f \frac{1}{l} dx$$

TABLE IX - Cont'd.

$$A_{31} = \pi \rho [(T_n - (c-e)P_n) \int_0^{\frac{3}{4}} (f_{n1}^{(11)} + x f_{n2}^{(11)}) dx + (T_n - (c-e)P_n) \left(\frac{df_{n1}^{(11)}}{dx} \right)_c \int_0^{\frac{3}{4}} b^2 dx] + \left(\frac{df_{n1}^{(11)}}{dx} \right)_c \int_0^{\frac{3}{4}} I_P dx$$

$$A_{32} = \pi \rho [(T_n - (c-e)P_n) \int_0^{\frac{3}{4}} (f_{n1}^{(11)} + x f_{n2}^{(11)}) dx + (T_n - (c-e)P_n) \left(\frac{df_{n1}^{(11)}}{dx} \right)_c \int_0^{\frac{3}{4}} b^2 dx] + \left(\frac{df_{n1}^{(11)}}{dx} \right)_c \int_0^{\frac{3}{4}} I_P dx$$

$$A_{33} = \pi \rho [(T_n - (c-e)P_n + T_s - (c)P_s) \int_0^{\frac{3}{4}} b^2 dx] + \int_0^{\frac{3}{4}} I_P dx$$

Notation in addition to that under COND. 1 :

f_1, f_2 subscript indexes fin, stabilizer respectively.

$f_{n1}^{(11)}, f_{n2}^{(11)}$ - side bending ^{angles etc} slope shape in mode i , of fuselage, at $\frac{3}{4}$ chord point of $\frac{3}{4}$ span fin station; $\left(\frac{df_{n1}^{(11)}}{dx} \right)_c$ same for side bending slope shape in mode i

$f_{ns}^{(11)}$ - angle of twist shape in mode i of fuselage at $\frac{3}{4}$ chord point of $\frac{3}{4}$ span stab. fin station

$\left(\frac{df_{n1}^{(11)}}{dx} \right)_w$ - side bending slope shape in mode i of fuselage station at wing elastic axis (Mode shapes shown in Table VIII)

mass data from Table III; dimensions: $b_f = 2.77$ ft, $c = c - e = .24$ ft

$b_s = 2.45$ ft stabilizer

COND. 10 Horizontal Tail

Cantilevered first coupled mode (35.8 rad/sec.) -

cantilevered second coupled mode (141.0 rad/sec.) -

elevator rotation (0 rad/sec.)

$A_{11}, A_{12}, A_{21}, A_{22}$ = same as for condition 5 using horizontal tail deflection shapes $f_{n1}^{(11)}, f_{n2}^{(12)}, f_{s1}^{(11)}, f_{s2}^{(12)}$ from TABLE VIII, mass data M_H, S_H, I_H from TABLE III,

$A_{13}, A_{23}, A_{31}, A_{32}, A_{33}$ = same as for condition 5 using $\sum I_E f_{n1}^{(11)}, \sum I_H f_{s1}^{(11)}$ for the mass terms, data from TABLE III & TABLE II, $b_f = 2.45$ ft, $c - e = .22$, $e = 0$

TABLE IX - Cont'd.

COND. 11 Horizontal Tail

Cantilevered first coupled mode (35.8 rad/sec.) -
cantilevered second coupled mode (144.6 rad/sec.)

$A_{11}, A_{12}, A_{21}, A_{22} =$ same as for condition 10.

$A_{13}, A_{23}, A_{31}, A_{32}, A_{33} = 0$ (four elements in determinant)

COND. 12 Vertical Tail

Cantilevered first coupled mode (66.5 rad/sec.) -
cantilevered second coupled mode (144.6 rad/sec.) -
rudder rotation (0 rad/sec.)

$A_{11}, A_{12}, A_{21}, A_{22} =$ same as for condition 5 using
vertical tail deflection shapes $f_h^{(1)}, f_h^{(2)}, f_x^{(1)}, f_x^{(2)}$ from
TABLE VIII, mass data M_v, S_v, I_v from TABLE IV

$A_{13}, A_{23}, A_{31}, A_{32}, A_{33} =$ same as for condition 5 using
 $\sum I_R f_x^{(1)}, \sum I_R f_x^{(2)}$ for the mass terms, data
from TABLE VIII & TABLE IV, $b_r = 2.77 \text{ ft}, e-e = .24,$
 $e = 0$

COND. 13 Vertical Tail

Cantilevered first coupled mode (66.5 rad/sec.) -
cantilevered second coupled mode (144.6 rad/sec.)

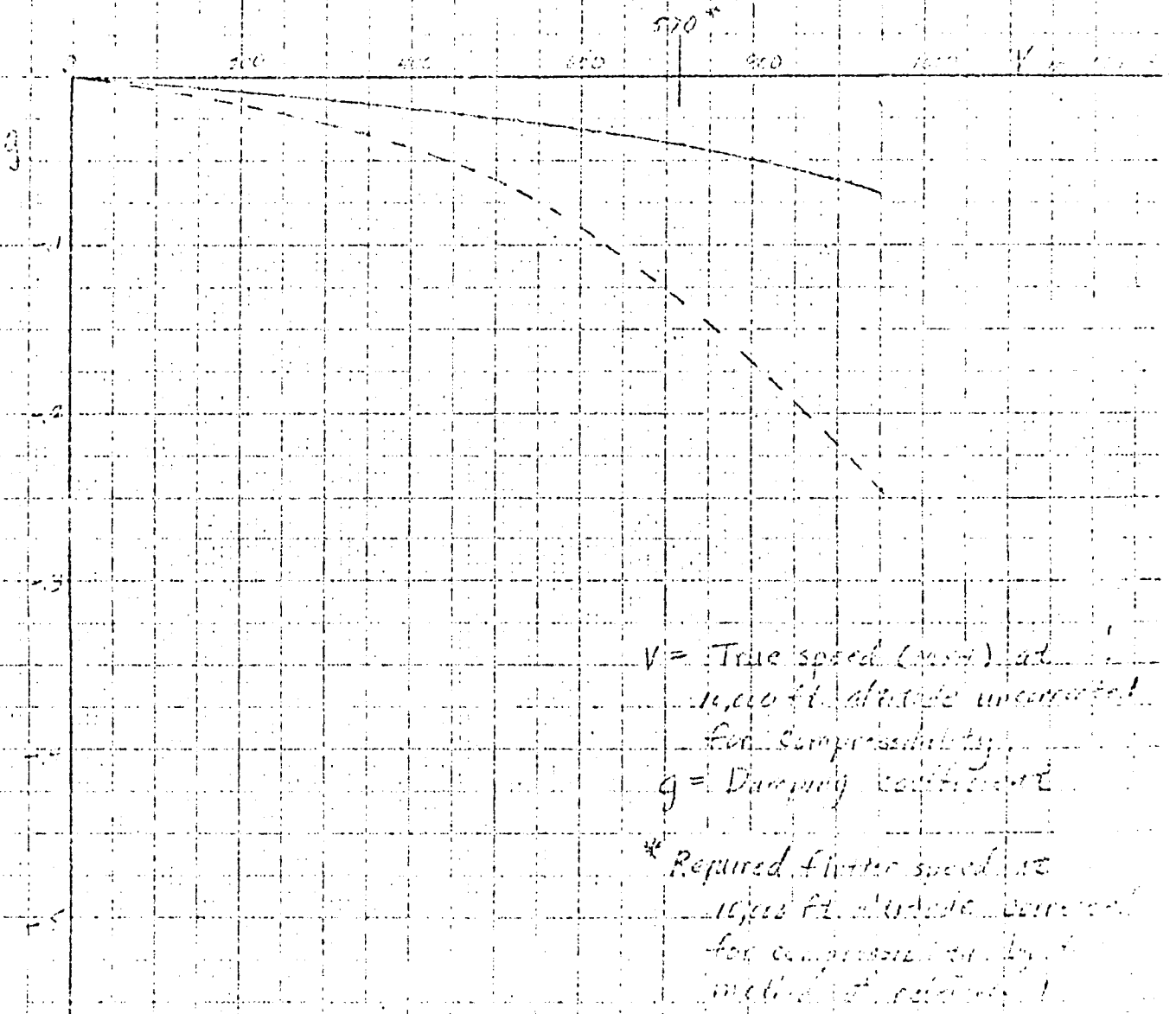
$A_{11}, A_{12}, A_{21}, A_{22} =$ same as for condition 12.

$A_{13}, A_{23}, A_{31}, A_{32}, A_{33} = 0$ (four elements in determinant)

CONSOLIDATED VELOCITY AERONAUTICAL CORPORATION
300 PLYMOUTH, OAKLAND, CALIFORNIA
FIGURE 7

DAMPING COEFFICIENT VS. SPEED CURVES
For Cond. 1 and Cond. 2

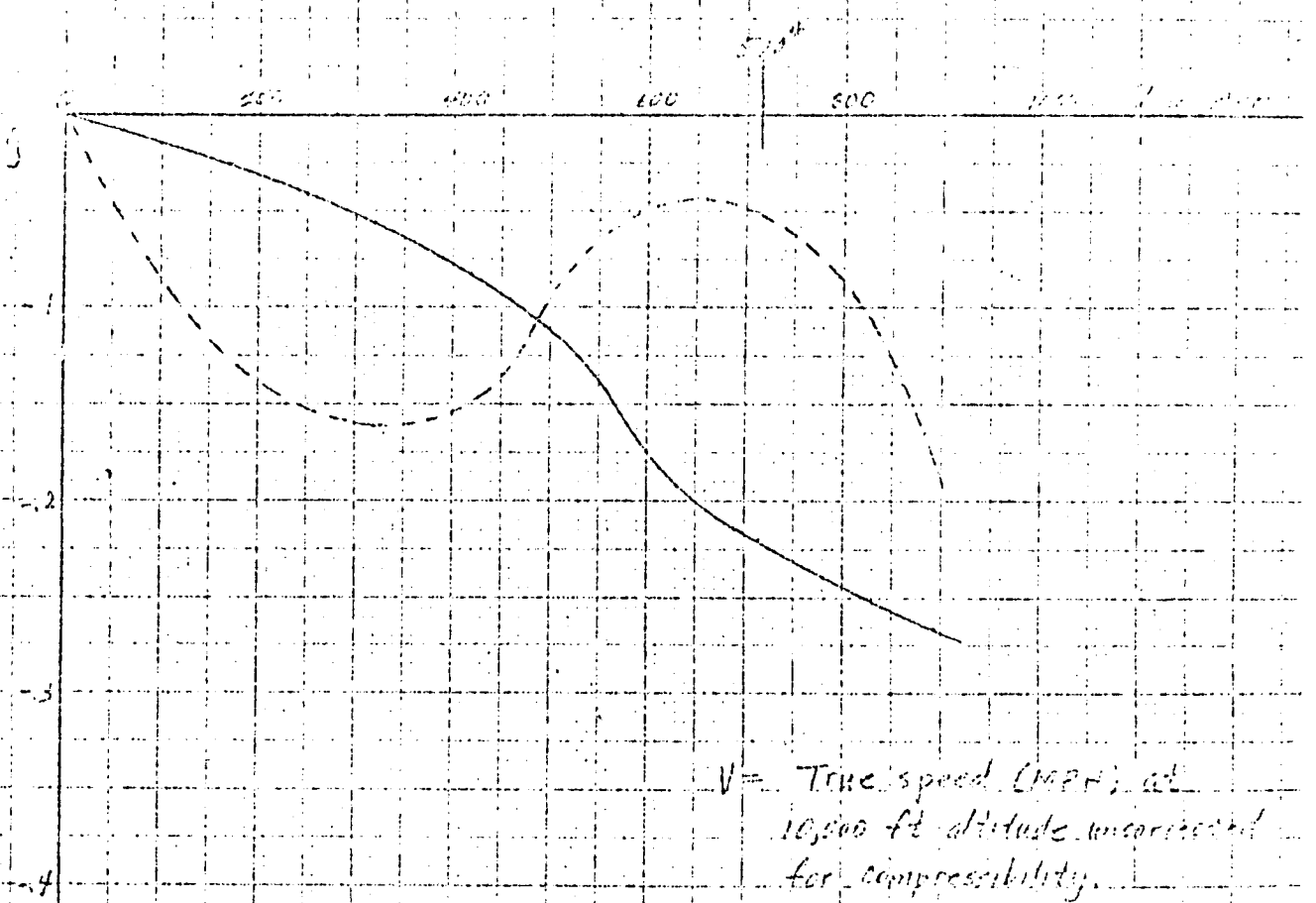
- Maximum Gross Weight (50,000 lbs.)
- COND. 1 ——— Symmetric first coupled wing mode (22.9 rad/sec)
 asymmetric second coupled wing mode (31.3 rad/sec)
 internal rotation (0 rad/sec)
- COND. 2 - - - - Symmetric first coupled wing mode (22.9 rad/sec)
 symmetric second coupled wing mode (31.3 rad/sec)



NATIONAL BUREAU OF STANDARDS
 DIVISION OF PHYSICS
 WASHINGTON, D. C. 20540

Flutter speed vs. $\frac{V}{V_{cr}}$ for $\frac{V}{V_{cr}} = 1.0$
 $\frac{V}{V_{cr}} = 1.0$
 $\frac{V}{V_{cr}} = 1.0$

- Maximum Circus Intensity (10,000 ft altitude)
 COND. 3 ——— Antisymmetric first coupled wing mode (1st) and the
 antisymmetric second coupled wing mode (2nd) and
 rotation (0 rad/sec.)
 COND. 4 ——— Antisymmetric first coupled wing mode (1st) and
 antisymmetric second coupled wing mode (2nd)



V = True speed (Mach) at
 10,000 ft altitude uncorrected
 for compressibility.

g = Damping coefficient

* Required flutter speed at
 10,000 ft altitude uncorrected
 for compressibility by the
 method of reference 1.

CONSOLIDATED MILITARY AERONAUTICAL DEVELOPMENT
 DIVISION, CALIFORNIA

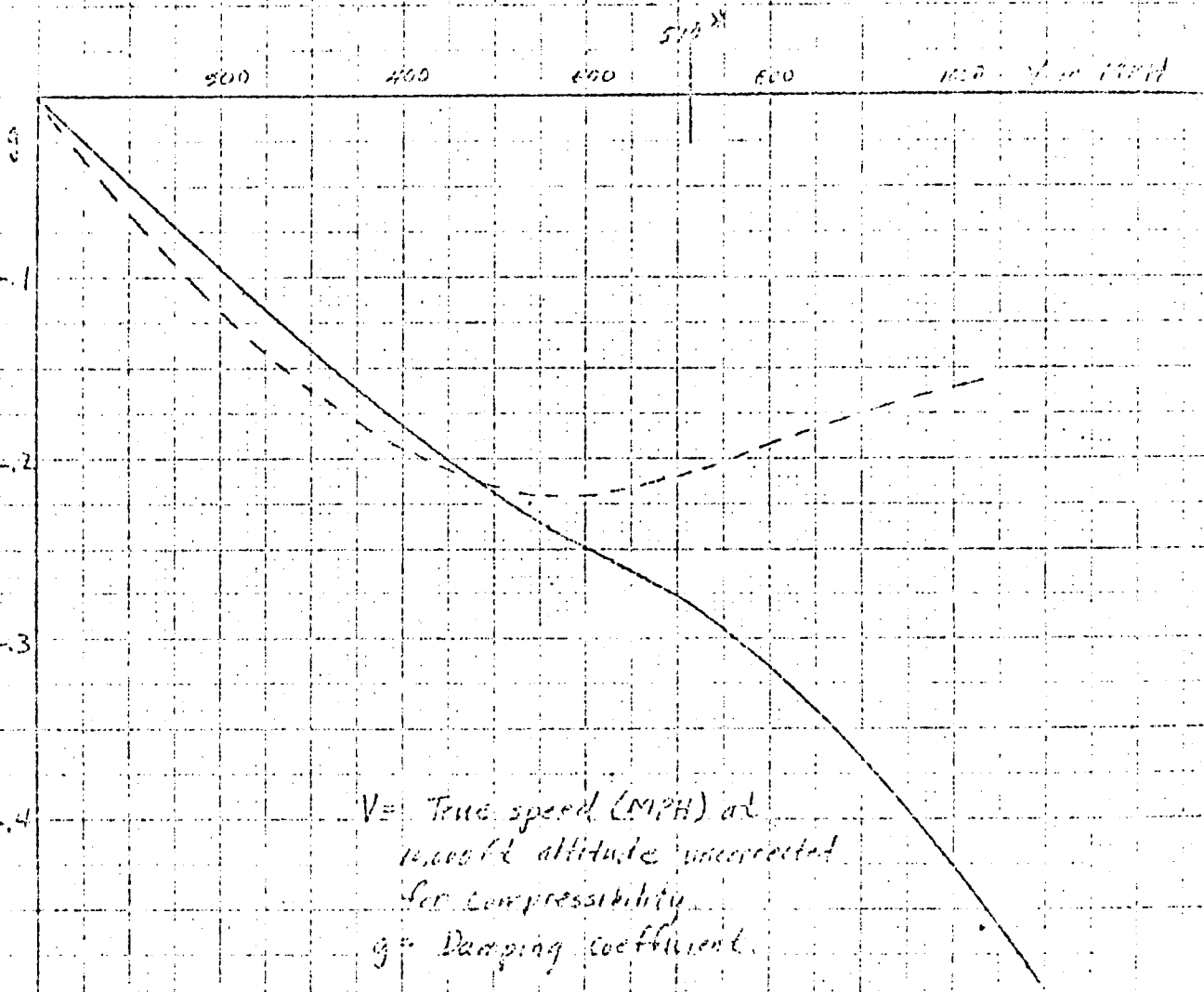
FIGURE 10

DAMPING COEFFICIENT VS. SPEED CURVES
 FOR COND. 7 AND COND. 8

Minimum Gross Weight (10,000 lbs)

COND. 7 — Antisymmetric first coupled wing mode (33% aileron antisymmetric second coupled wing mode (45% aileron rotation (aileron))

COND. 8 — Antisymmetric first coupled wing mode (33% antisymmetric second coupled wing mode (45% aileron rotation (aileron))



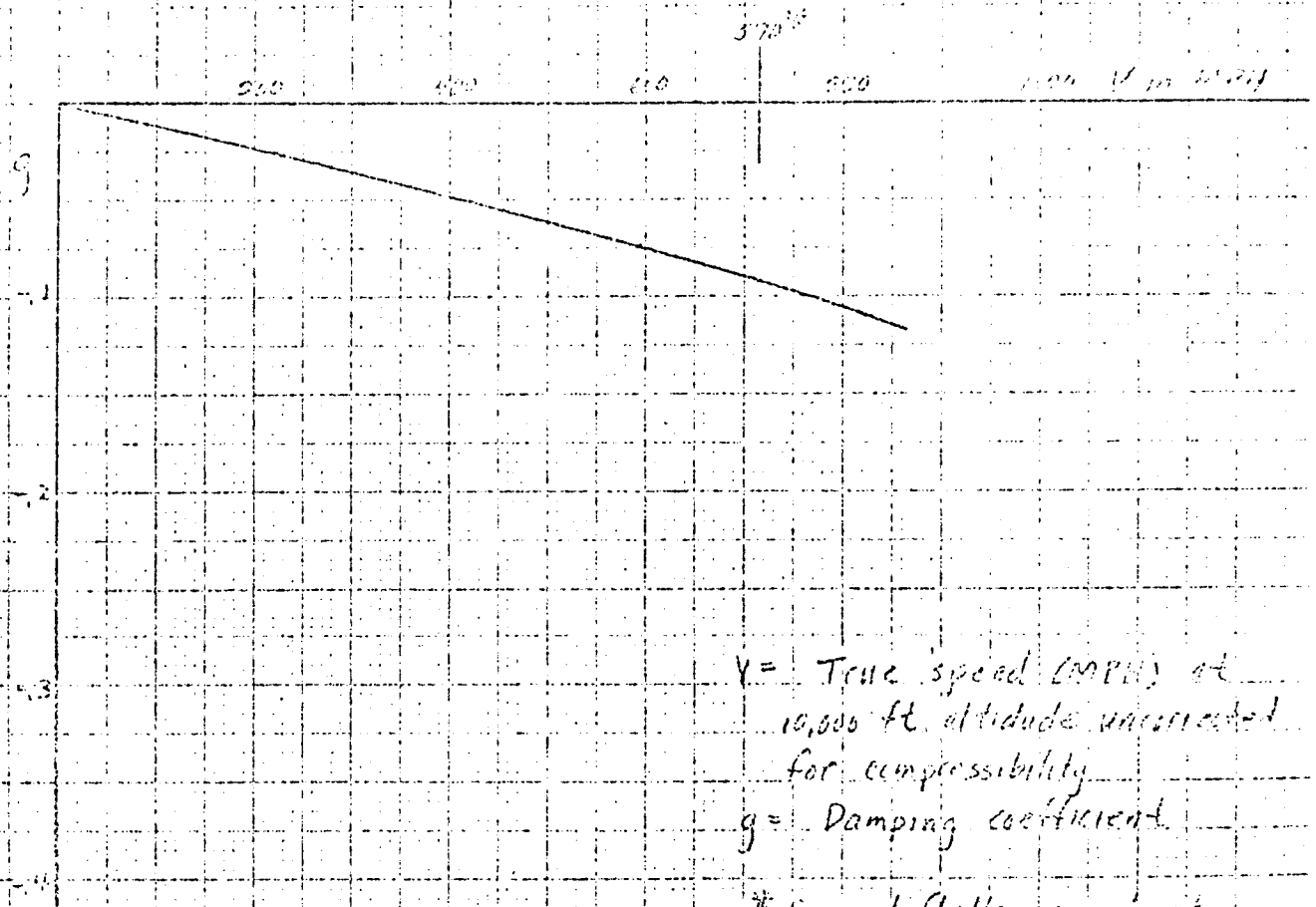
$V =$ True speed (MPH) at 10,000 ft altitude uncorrected for compressibility.
 $g =$ Damping coefficient.

$V_{crit} =$ Reported flutter speed at 10,000 ft altitude uncorrected for compressibility by the method of reference 1.

CONSOLIDATED REPORT TO AIRCRAFT CORPORATION
 SERIAL 10-722-11

DAMPING COEFFICIENT VS SPEED CURVE
 FOR COND. 3

Maximum Gross Weight Fuselage (40,000 lbs.)
 Lateral first coupled fuselage mode (370 rad/sec)
 lateral second coupled fuselage mode (580 rad/sec)
 rudder rotation (0 rad/sec)



V = True speed (MPH) at
 10,000 ft. altitude uncorrected
 for compressibility
 g = Damping coefficient

* Reported flutter speed at
 10,000 ft. altitude corrected
 for compressibility by the
 method of reference 1.

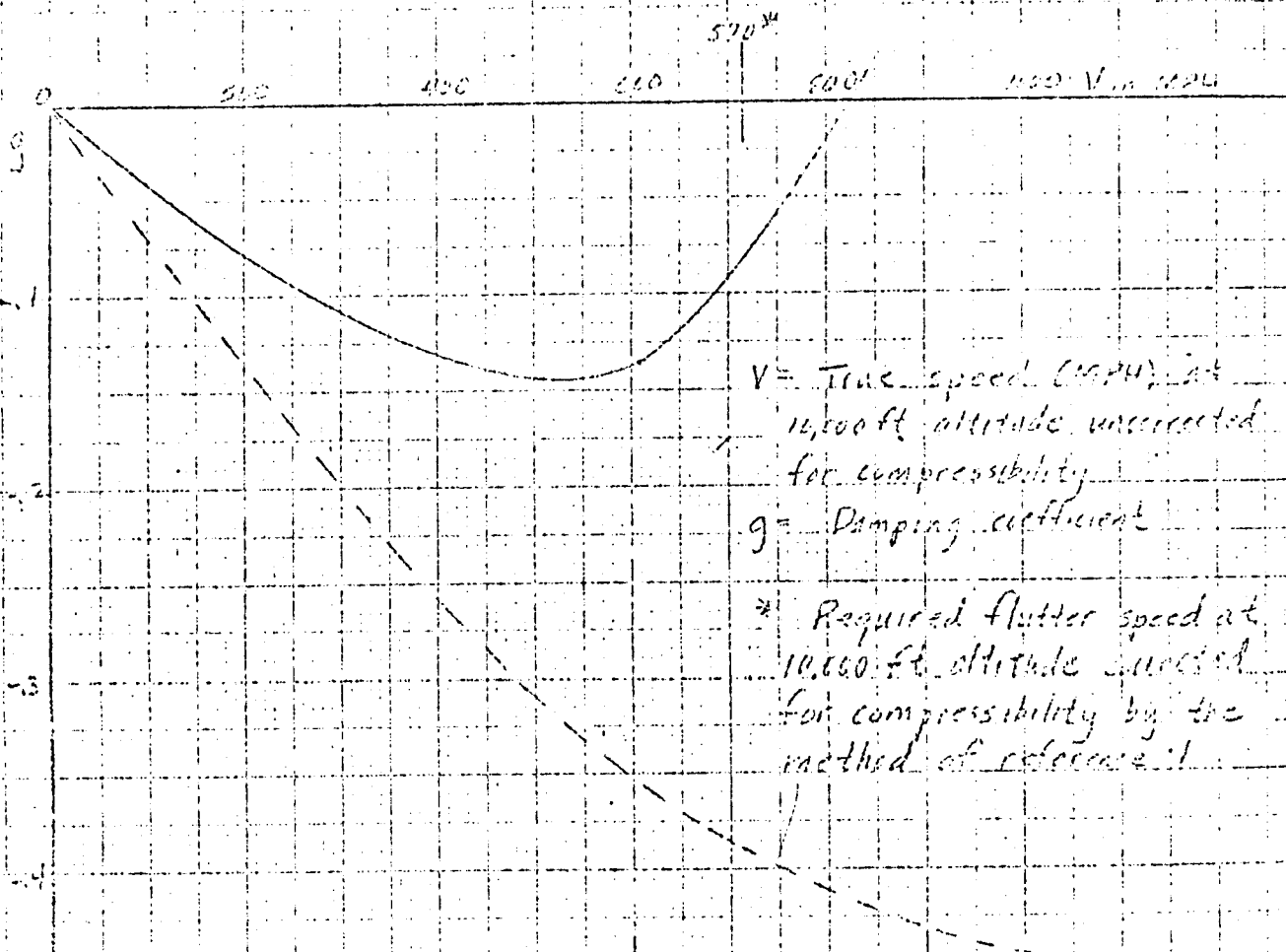
No. 25041. Do not use for classification. Form 7-54
 (Rev. 7-54)

DAMPING COEFFICIENT VS SPEED CURVE
FOR COND. 10 AND COND. 11

Horizontal Tail

COND. 10 ——— Cantilevered first coupled mode (55.2 rad/sec),
 cantilevered second coupled mode (114.0 rad/sec),
 elevator rotation (6.0 rad/sec)

COND. 11 - - - Cantilevered first coupled mode (55.2 rad/sec),
 cantilevered second coupled mode (114.0 rad/sec)



V = True speed (ft/min), at
 10,000 ft altitude uncorrected
 for compressibility

g = Damping coefficient

* Required flutter speed at
 10,000 ft altitude uncorrected
 for compressibility by the
 method of reference 1

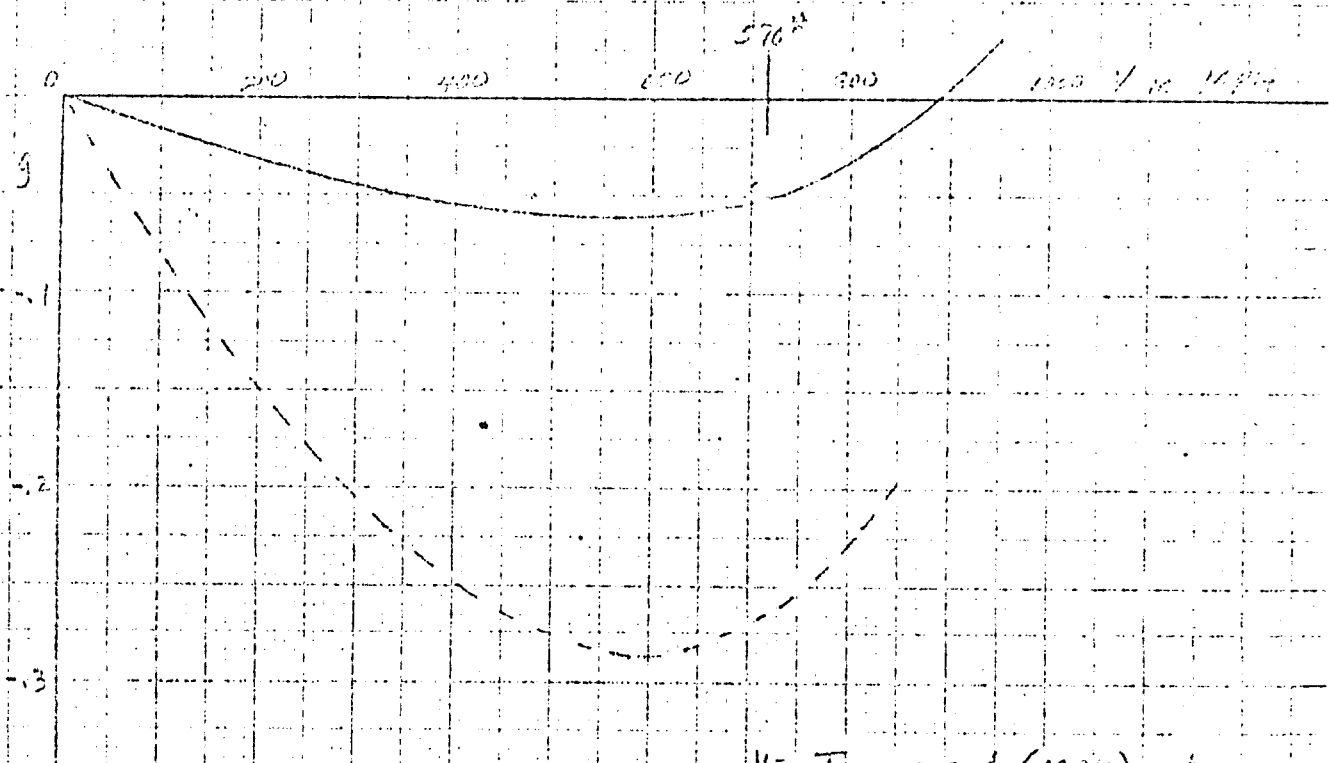
FIGURE 13

DAMPING COEFFICIENT VS SPEED CURVE
FOR COND. 12 AND COND. 13

Vertical Tail

COND. 12 ——— Cantilevered first coupled mode (11.5 rad/sec);
cantilevered second coupled mode (1.94 rad/sec);
rudder rotation (0 rad/sec)

COND. 13 - - - Cantilevered first coupled mode (16.5 rad/sec);
cantilevered second coupled mode (1.44 rad/sec)



V = True speed (IAFH) at
10,000 ft altitude uncorrected
for compressibility

g = Damping coefficient

* Required flutter speed at
10,000 ft altitude corrected
for compressibility by the
method of reference 1

0-1000 1000 1000

Discussion

Examination of the results in figures 7 to 11 indicates that the local 340 turbo-propeller airplane is more prone to flutter up to the critical flutter speed of 170 mph. These data are considered to apply to the turbo-propeller engine version of the local 340 airplane, since the effect of the change of power plant leads to only minor changes in the mass and stiffness properties of the wing. A variation of the amount of aerodynamic control surface inboard of the midspan is expected of the turbo-propeller engine version since that the turbo-propeller version of the local 340, however, due to the small variations involved the difference in results are considered to be within the accuracy of the present analysis.

CONFIDENTIAL
PROPERTY OF
GENERAL ELECTRIC COMPANY

CONFIDENTIAL - GENERAL ELECTRIC COMPANY
SAN DIEGO DIVISION

DATE 12
REVISION 10-10-50
PAGE 10
DATE (10-10-50)

REFERENCES

1. "Application of Three-Dimensional Flutter Theory to Rigid Structures", Army Air Force Technical Report 3472, Wright-Field, Dayton, Ohio, July 1942.
2. "Vibration Analysis", N. O. Myklestad, McGraw-Hill Book Co., Inc. 1944 pp. 201, 215.
3. "Calculation of Coupled Vibration Modes and Frequencies of Aircraft", L. Dillin, paper presented at ASEE meeting for Applied Mechanics, Stanford University, June 1951.